Hindawi
Mathematical Problems in Engineering
Volume 2018, Article ID 9435761, 12 pages
https://doi.org/10.1155/2018/9435761

Research Article

Modified Empirical Eigenfunctions and Its Applications for Model Reduction of Nonlinear Spatiotemporal Systems

Mian Jiang, Shuangqi Liu, and Jigang Wu

Hunan Provincial Key Laboratory of Health Maintenance for Mechanical Equipment, Hunan University of Science and Technology, XiangTan 411201, China

Correspondence should be addressed to Mian Jiang; mjiang@cvm.ac.cn

Received 16 May 2018; Revised 13 September 2018; Accepted 27 September 2018; Published 14 November 2018

Academic Editor: Jose Vicente Salcedo

Model reduction can greatly reduce complexity and difficulty of control design for spatiotemporal systems (STS) in engineering applications. Empirical eigenfunctions (EEFs) are widely used for the model reduction of spatiotemporal systems, however, truncation of higher modes may describe the behaviours of nonlinear spatiotemporal systems inaccurately. In this paper, modified EEFs are proposed and applied to model reduction of nonlinear spatiotemporal systems. Modified EEFs are obtained via modifying the weights matrix in the method of snapshots, which can be rewritten as linear combinations of initial EEFs. The coefficient matrix for combinations is computed according to the nonlinear temporal dynamics of STSs. Thus, the effects of higher modes are considered into modified EEFs with less computational requirements. The reduced model can give a more accurate description for behaviours of the system. The performance of the proposed method is further proved theoretically, and a numerical example demonstrates the effectiveness of the proposed method.

1. Introduction

With their nonuniformly distributed dynamics in space, many engineering problems belong to a class of nonlinear spatiotemporal systems (STSs) or distributed parameter systems (DPSs). Their infinite-dimensional spatiotemporal coupling and complex nonlinear behaviours make modelling, system analysis, numerical simulations and control design very difficult. Thus, model reduction for nonlinear STSs at a reasonable cost and accuracy has a great significance in practical engineering applications. Empirical eigenfunctions (EEFs) identified by proper orthogonal decomposition (POD) [1] are widely used as global spatial basis functions in advanced methods for model reduction of nonlinear STSs [2–8]. Modes obtained from POD can be calculated quite easily as the solutions of an eigenvalue problem involving second-order correlation tensors. When establishing a low-dimensional dynamic model, few POD modes are used to capture the dominant dynamics of nonlinear STSs according to the energetic optimality. However, the traditional POD is a linear dimension reduction (i.e., linear projection and linear reconstruction) method, and it produces a linear approximation to the measured data with nonlinear spatiotemporal structure, which may not guarantee the assumption that minor components do not contain important information. As a result, truncation of higher modes with small "energies" may have great influences on accuracy of the reduced model [9]. Without considering the effects of higher modes, the reduced dynamic model will give an inaccurate description for the spatiotemporal dynamic behaviours of STSs.

This situation has been addressed in some literatures. With more computational power for training, the nonlinear dimension reduction method named nonlinear POD was developed for nonlinear problems to retain more information using fewer components. The nonlinear POD has a more powerful capability of dimension reduction than the traditional POD for nonlinear systems. This method has been widely used to deal with the nonlinear dimension reduction problems in the field of machine learning, image processing and pattern recognition. Examples include principal curves, multilayer autoassociative neural networks, kernel function approach, and radial basis function(RBF)

networks. ISOMAP-based spatiotemporal modelling [10] and LLE- based nonlinear spatiotemporal modelling [11] are also proposed to improve the performance of POD-based reduced mode in recent years. However, these methods mainly focus on the reduction and analysis of multivariate time series or the order reduction of DPSs with no analytical models [12].

To deal with the inaccuracy of traditional POD method, some literatures related to fluid dynamics are also given. In 1990s, Aubry [13] and Armbruster [14] respectively pointed out that the reduced models using the first several EEFs can have difficulties reproducing behaviours dominated by irregular transitions between different dynamical states. In 2003, Noack [15] had found that the low-dimensional Galerkin model by traditional POD method cannot approximate the transient behaviours of flow around a circular cylinder well. He introduced a new "shift mode" to improve the performance of the low-dimensional model, which incorporates the steady solution in the POD framework. In 2010, Sengupta [16] built the relationship of instability modes with POD modes in the study of global spatiotemporal nonlinear instabilities for flow past a cylinder. In recent years, the effects of higher modes are highlighted [17] and discussed [18] in the field of fluid dynamic systems. Some approaches such as spectral viscosity method [19] and variational multiscale model [20] based on the traditional POD are developed to deal with the problems. However, some additional empirical parameters are introduced into these methods for model correction, and their optimizations depend on specific problems. Another important method to improve the accuracy and dynamical system properties of POD-based reduced order models is sensitivity-based enhancement of modes [21–23], which uses sensitivity analysis (SA) to include the flow and shape parameters influence during the basis selection process to develop more robust reduced order models for varying parameters. It has shown promising results for parametric variation due to richness in the eigenfunctions and presents modified eigenfunctions though in a different setting.

To introduce the effects of higher modes into the POD-based reduced model, nonlinear closure modelling [24, 25], nonlinear Galerkin method, and improved EEFs [26–28] are proposed to improve the model reduction performance. The higher modes contain relatively low energies but play a vital role in the overall dynamics of complex flows. Nonlinear closure modelling [24, 25] enhances the performance of POD-based reduced order model at low computational cost. Though it still remains a challenging task for 3D turbulent flows, closure modelling already shows promising results for Burgers' equation and the Navier-Stokes equations. Nonlinear Galerkin method considers the effects of higher modes via approximate inertial manifolds (AIM) [26] and is used to approximate the nonlinear DPSs for fluids systems. The space spanned by EEFs is split into two subspaces and the interactions between lower and higher modes are built via AIM to compensate the modelling accuracy. However, the calculations for AIM in this method are theoretically complex and computational power-consuming. The improved EEFs [28] use the transformation for initial EEFs from traditional POD to derive a new set of basis functions, while the transformation matrix is obtained according to balanced truncation method for an approximated linear temporal system of a STS. This method introduces the dynamical information of higher modes into new basis functions to derive the reduced model. Because the transformation matrix is obtained from the linear approximation for nonlinear dynamics of the STS, this method can be improved by utilizing the global nonlinear dynamics directly to calculate the matrix.

In this paper, modified EEFs are developed and applied to model reduction of nonlinear STSs. The EEFs are modified by introducing an extra weights matrix into the method of snapshots, which is commonly used to calculate the EEFs in traditional POD. This procedure transforms the derivation of modified EEFs to linear combinations of initial EEFs, where the coefficients matrix is computed directly according to the nonlinear temporal dynamics of STSs. Thus, the effects of higher modes are considered into modified EEFs and give a better accuracy of the reduced-order model. The effectiveness of the proposed method is proved theoretically. This method requires less computational consumption and a numerical example shows that it has a better performance than the improved EEFs based modelling [28].

2. EEFs Based Model Reduction for STSs

Assuming that a kind of nonlinear STSs can be governed by a partial differential equation (PDE) with the following state description:

$$\frac{\partial \boldsymbol{X}}{\partial \boldsymbol{t}} = \mathscr{A}\boldsymbol{X} + \mathscr{B}\boldsymbol{U} + \mathscr{F}\left(\boldsymbol{X}, \frac{\partial \boldsymbol{X}}{\partial \boldsymbol{z}}, \cdots, \boldsymbol{U}, \frac{\partial \boldsymbol{U}}{\partial \boldsymbol{z}}, \cdots\right) \quad (1)$$

subject to a number of boundary and initial conditions. In (1), $\boldsymbol{X} = \boldsymbol{X}(\boldsymbol{z}, \boldsymbol{t})$ denotes the vector of state variable, where $\boldsymbol{t} \in [0, \infty)$ is the time variable, $\boldsymbol{z} \in \Omega$ is the spatial coordinate, and only one spatial-dimension is considered here. $\boldsymbol{U} = \boldsymbol{U}(\boldsymbol{z}, \boldsymbol{t})$ denotes the vector of manipulated spatio-temporal inputs, where $\boldsymbol{U} = \sum_{i=1}^{m} \boldsymbol{h_i}(\boldsymbol{z})\boldsymbol{u_i}(\boldsymbol{t})$ and $\boldsymbol{u_i}(\boldsymbol{t})$ is the ith temporal signal with certain spatial distribution $\boldsymbol{h_i}(\boldsymbol{z})$. $\mathscr{A}$ and $\mathscr{B}$ are two linear operators that involve linear spatial derivatives on the state variable and spatiotemporal input. $\partial \boldsymbol{X}/\partial \boldsymbol{z}$ and $\partial \boldsymbol{U}/\partial \boldsymbol{z}$ denote the partial derivatives of $\boldsymbol{X}$ and $\boldsymbol{U}$, respectively. $\mathscr{F}$ is a nonlinear function containing spatial derivatives for $\boldsymbol{X}$ and $\boldsymbol{U}$. A scalar product is defined on spatial domain Ω introduced in the phase space of (1), which is given by $(\boldsymbol{f}(\boldsymbol{z}), \boldsymbol{g}(\boldsymbol{z}))_\Omega = \int_\Omega \boldsymbol{f}(\boldsymbol{z})\boldsymbol{g}(\boldsymbol{z})\boldsymbol{dz}$.

The spatiotemporal variable $\boldsymbol{X}(\boldsymbol{z}, \boldsymbol{t})$ is assumed to be expanded onto the set of EEFs $\{\varphi_1(\boldsymbol{z}), \varphi_2(\boldsymbol{z}), \cdots, \varphi_N(\boldsymbol{z})\}$ (the computational details are given in Appendix) with corresponding temporal coefficients

$$\boldsymbol{X}(\boldsymbol{z}, \boldsymbol{t}) = \sum_{\boldsymbol{i}=1}^{\boldsymbol{N}} \boldsymbol{x_i}(\boldsymbol{t})\, \varphi_{\boldsymbol{i}}(\boldsymbol{z}). \quad (2)$$

Suppose that the spatial-temporal output $\boldsymbol{Y}(\boldsymbol{z}, \boldsymbol{t})$ is measured at $\boldsymbol{M}$ spatial locations. Substituting the expansion (2) into (1) and taking the inner product with $\varphi_{\boldsymbol{i}}(\boldsymbol{z})$ (orthogonality), the integration of equation will give a finite-dimensional

nonlinear ordinary differential equation (ODE) system in a general form as follows:

$$\begin{aligned} \dot{\boldsymbol{x}}(t) &= \boldsymbol{A}\boldsymbol{x}(t) + \boldsymbol{B}\boldsymbol{u}(t) + \boldsymbol{f}(\boldsymbol{x}(t), \boldsymbol{u}(t)) \\ \boldsymbol{y}(t) &= \boldsymbol{S}\boldsymbol{x}(t) \end{aligned} \tag{3}$$

where $\boldsymbol{x}(t) = [x_1(t), x_2(t), \cdots, x_N(t)]^T$ with $\boldsymbol{x_i}(t)$ is the temporal coefficient and $\boldsymbol{y}(t) = [\boldsymbol{Y}(z_1, t), \boldsymbol{Y}(z_2, t), \cdots, \boldsymbol{Y}(z_M, t)]^T$ with $\boldsymbol{Y}(\boldsymbol{z_i}, \boldsymbol{t})$ denotes the measured output on the location $\boldsymbol{z_i}$.

The matrices and the nonlinear terms in (3) are given as follows:

$$\begin{aligned} \boldsymbol{A} &= \left\{\boldsymbol{A_{ij}}\right\}_{N\times N}, \quad \boldsymbol{A_{ij}} = \left(\mathscr{A}\varphi_j(\boldsymbol{z}), \varphi_i(\boldsymbol{z})\right)_\Omega, \\ \boldsymbol{B} &= \left\{\boldsymbol{B_{ij}}\right\}_{N\times N}, \quad \boldsymbol{B_{ij}} = \left(\mathscr{B}\varphi_j(\boldsymbol{z}), \varphi_i(\boldsymbol{z})\right)_\Omega, \\ \boldsymbol{S} &= \left\{\boldsymbol{S_{ij}}\right\}_{M\times N}, \quad \boldsymbol{S_{ij}} = \varphi_j(\boldsymbol{z_i}), \end{aligned} \tag{4}$$

where $\boldsymbol{z}_1, \boldsymbol{z}_2, \cdots, \boldsymbol{z}_M$ are the spatial locations.

$$\begin{aligned} \boldsymbol{f}(\boldsymbol{x}(t), \boldsymbol{u}(t)) = [&\boldsymbol{f}_1(\boldsymbol{x}(t), \boldsymbol{u}(t)), \boldsymbol{f}_2(\boldsymbol{x}(t), \boldsymbol{u}(t)), \cdots, \\ &\boldsymbol{f}_N(\boldsymbol{x}(t), \boldsymbol{u}(t))]^T \end{aligned} \tag{5}$$

is the vector of nonlinear terms with

$$\begin{aligned} &\boldsymbol{f_i}(\boldsymbol{x}(t), \boldsymbol{u}(t)) \\ &\quad = \left(\mathscr{F}\left(\boldsymbol{X}, \frac{\partial \boldsymbol{X}}{\partial \boldsymbol{z}}, \cdots, \boldsymbol{U}, \frac{\partial \boldsymbol{U}}{\partial \boldsymbol{z}}, \cdots\right), \varphi_i(\boldsymbol{z})\right)_\Omega. \end{aligned} \tag{6}$$

The EEFs-based modeling could be one of the most commonly used DPS modeling methods. It has been applied to system analysis, model reduction, simulations for many complex processes. However, truncation of higher modes with critical dynamics information will greatly influence the model reduction performance in many situations.

3. Modified EEFs and Its Applications for Model Reduction

3.1. The Modified Principle. It is assumed that $\{\boldsymbol{Y}_{(l)}(\boldsymbol{z})\}$ denote the ensemble data on space location z in the method of snapshots, where $\boldsymbol{l}$ is the time sampling point. EEFs is usually calculated in the situation that $\boldsymbol{N_{Tim}}$, the number of grid points for each snapshots, is much larger than N, the total number of the ensemble $\{\boldsymbol{Y}_{(l)}(\boldsymbol{z})\}$. It is computationally advantageous to transform the calculation of EEFs as a $\boldsymbol{N}\times\boldsymbol{N}$ eigenvalue problem. Thus, the $\boldsymbol{n}$th EEFs of the eigenvalue problem (Appendix, (A.6)) can be reconstructed from the coefficients $\boldsymbol{c_j^n}$ and eigenvalue λ_n via

$$\varphi_{\boldsymbol{n}}(\boldsymbol{z}) = \frac{1}{\lambda_{\boldsymbol{n}}\boldsymbol{N}}\left[\boldsymbol{c}_1^{\boldsymbol{n}} \ \cdots \ \boldsymbol{c}_{\boldsymbol{N}}^{\boldsymbol{n}}\right]\begin{bmatrix}\boldsymbol{Y}_{(1)}(\boldsymbol{z}) \\ \vdots \\ \boldsymbol{Y}_{(N)}(\boldsymbol{z})\end{bmatrix}. \tag{7}$$

The maximum number of the EEFs in the eigenvalue problem is $\boldsymbol{N}$, which can be given as follows:

$$\begin{bmatrix}\varphi_1(\boldsymbol{z}) \\ \vdots \\ \varphi_N(\boldsymbol{z})\end{bmatrix} = \frac{1}{\boldsymbol{N}}\boldsymbol{C}\begin{bmatrix}\boldsymbol{Y}_{(1)}(\boldsymbol{z}) \\ \vdots \\ \boldsymbol{Y}_{(N)}(\boldsymbol{z})\end{bmatrix} \tag{8}$$

where

$$\boldsymbol{C} = \begin{bmatrix}\dfrac{\boldsymbol{c}_1^1}{\lambda_1} & \cdots & \dfrac{\boldsymbol{c}_N^1}{\lambda_1} \\ \vdots & & \vdots \\ \dfrac{\boldsymbol{c}_1^N}{\lambda_N} & \cdots & \dfrac{\boldsymbol{c}_N^N}{\lambda_N}\end{bmatrix}. \tag{9}$$

If the first $\boldsymbol{k}$ EEFs in (8) are truncated for model reduction of STSs, then we have

$$\begin{bmatrix}\varphi_1(\boldsymbol{z}) \\ \vdots \\ \varphi_{\boldsymbol{k}}(\boldsymbol{z})\end{bmatrix} = \frac{1}{\boldsymbol{N}}\boldsymbol{C}^{(1)}\begin{bmatrix}\boldsymbol{Y}_{(1)}(\boldsymbol{z}) \\ \vdots \\ \boldsymbol{Y}_{(N)}(\boldsymbol{z})\end{bmatrix}, \tag{10}$$

$$\begin{bmatrix}\varphi_{\boldsymbol{k}+1}(\boldsymbol{z}) \\ \vdots \\ \varphi_{\boldsymbol{N}}(\boldsymbol{z})\end{bmatrix} = \frac{1}{\boldsymbol{N}}\boldsymbol{C}^{(2)}\begin{bmatrix}\boldsymbol{Y}_{(1)}(\boldsymbol{z}) \\ \vdots \\ \boldsymbol{Y}_{(N)}(\boldsymbol{z})\end{bmatrix}, \tag{11}$$

where $\boldsymbol{k} \le \boldsymbol{N}$ and

$$\boldsymbol{C}^{(1)} = \begin{bmatrix}\dfrac{\boldsymbol{c}_1^1}{\lambda_1} & \cdots & \dfrac{\boldsymbol{c}_N^1}{\lambda_1} \\ \vdots & & \vdots \\ \dfrac{\boldsymbol{c}_1^{\boldsymbol{k}}}{\lambda_{\boldsymbol{k}}} & \cdots & \dfrac{\boldsymbol{c}_N^{\boldsymbol{k}}}{\lambda_{\boldsymbol{k}}}\end{bmatrix}, \tag{12}$$

$$\boldsymbol{C}^{(2)} = \begin{bmatrix}\dfrac{\boldsymbol{c}_1^{\boldsymbol{k}+1}}{\lambda_{\boldsymbol{k}+1}} & \cdots & \dfrac{\boldsymbol{c}_N^{\boldsymbol{k}+1}}{\lambda_{\boldsymbol{k}+1}} \\ \vdots & & \vdots \\ \dfrac{\boldsymbol{c}_1^{\boldsymbol{N}}}{\lambda_{\boldsymbol{N}}} & \cdots & \dfrac{\boldsymbol{c}_N^{\boldsymbol{N}}}{\lambda_{\boldsymbol{N}}}\end{bmatrix}. \tag{13}$$

However, truncation of high modes in (8) may have a great influence on performance of the EEF-based reduced model. The solution of obtained nonlinear dynamic systems will have high-sensitive dependence on perturbations, a slight perturbation (e.g., inappropriate truncation of higher modes) would lead to topological changes of the dynamic system. Thus, the modified EEFs are given by adding an extra weight matrix $\boldsymbol{Q}$ into (8)

$$\begin{bmatrix}\phi_1(\boldsymbol{z}) \\ \vdots \\ \phi_{\boldsymbol{k}}(\boldsymbol{z})\end{bmatrix} = \frac{1}{\boldsymbol{N}}\boldsymbol{Q}\boldsymbol{C}\begin{bmatrix}\boldsymbol{Y}_{(1)}(\boldsymbol{z}) \\ \vdots \\ \boldsymbol{Y}_{(N)}(\boldsymbol{z})\end{bmatrix}, \tag{14}$$

where

$$\boldsymbol{Q} = \begin{bmatrix} \boldsymbol{Q}_{11} & \cdots & \boldsymbol{Q}_{1N} \\ \vdots & & \vdots \\ \boldsymbol{Q}_{k1} & \cdots & \boldsymbol{Q}_{kN} \end{bmatrix}. \tag{15}$$

The modified EEFs (14) can be rewritten as follows:

$$\begin{aligned} \begin{bmatrix} \phi_1(\boldsymbol{z}) \\ \vdots \\ \phi_k(\boldsymbol{z}) \end{bmatrix} &= \frac{1}{N} \begin{bmatrix} \boldsymbol{Q}^{(1)} & \boldsymbol{Q}^{(2)} \end{bmatrix} \begin{bmatrix} \boldsymbol{C}^{(1)} \\ \boldsymbol{C}^{(2)} \end{bmatrix} \begin{bmatrix} \boldsymbol{Y}_{(1)}(\boldsymbol{z}) \\ \vdots \\ \boldsymbol{Y}_{(N)}(\boldsymbol{z}) \end{bmatrix} \\ &= \frac{1}{N} \boldsymbol{Q}^{(1)} \boldsymbol{C}^{(1)} \begin{bmatrix} \boldsymbol{Y}_{(1)}(\boldsymbol{z}) \\ \vdots \\ \boldsymbol{Y}_{(N)}(\boldsymbol{z}) \end{bmatrix} \\ &\quad + \frac{1}{N} \boldsymbol{Q}^{(2)} \boldsymbol{C}^{(2)} \begin{bmatrix} \boldsymbol{Y}_{(1)}(\boldsymbol{z}) \\ \vdots \\ \boldsymbol{Y}_{(N)}(\boldsymbol{z}) \end{bmatrix} \end{aligned} \tag{16}$$

where

$$\begin{aligned} \boldsymbol{Q}^{(1)} &= \begin{bmatrix} \boldsymbol{Q}_{11} & \cdots & \boldsymbol{Q}_{1k} \\ \vdots & & \vdots \\ \boldsymbol{Q}_{k1} & \cdots & \boldsymbol{Q}_{kk} \end{bmatrix}, \\ \boldsymbol{Q}^{(2)} &= \begin{bmatrix} \boldsymbol{Q}_{1k+1} & \cdots & \boldsymbol{Q}_{1N} \\ \vdots & & \vdots \\ \boldsymbol{Q}_{kk+1} & \cdots & \boldsymbol{Q}_{kN} \end{bmatrix}. \end{aligned} \tag{17}$$

Substituting (10) and (11) into (16), the modified EEFs are obtained from the first $\boldsymbol{k}$ EEFs and truncated higher modes as follows:

$$\begin{bmatrix} \phi_1(\boldsymbol{z}) \\ \vdots \\ \phi_k(\boldsymbol{z}) \end{bmatrix} = \boldsymbol{Q}^{(1)} \begin{bmatrix} \varphi_1(\boldsymbol{z}) \\ \vdots \\ \varphi_k(\boldsymbol{z}) \end{bmatrix} + \boldsymbol{Q}^{(2)} \begin{bmatrix} \varphi_{k+1}(\boldsymbol{z}) \\ \vdots \\ \varphi_N(\boldsymbol{z}) \end{bmatrix}. \tag{18}$$

It is clear that the weights of initial EEFs in (8) are changed from $\boldsymbol{C}$ to $\boldsymbol{QC}$. And we can find that each modified EEFs is the linear combination of initial $\boldsymbol{N}$ EEFs as follows:

$$\phi_{\boldsymbol{i}}(\boldsymbol{z}) = \boldsymbol{Q}_{\boldsymbol{i}1}\varphi_1(\boldsymbol{z}) + \boldsymbol{Q}_{\boldsymbol{i}2}\varphi_2(\boldsymbol{z}) + \cdots + \boldsymbol{Q}_{\boldsymbol{i}N}\varphi_N(\boldsymbol{z}), \tag{19}$$

where $\boldsymbol{i} = 1, 2, \cdots, \boldsymbol{k}$. This relationship of modified EEFs and initial EEFs can be rewritten in the following:

$$\begin{aligned} &\{\phi_1(\boldsymbol{z}), \phi_2(\boldsymbol{z}), \cdots, \phi_k(\boldsymbol{z})\} \\ &\quad = \{\varphi_1(\boldsymbol{z}), \varphi_2(\boldsymbol{z}), \cdots, \varphi_N(\boldsymbol{z})\} \boldsymbol{Q}^T \end{aligned} \tag{20}$$

where $\boldsymbol{k} < \boldsymbol{n}$ and $\boldsymbol{Q}$ denotes the matrix of combined coefficients. The modified EEFs is transformed from initial EEFs using (20), which number is smaller than that of initial EEFs. This indicates that new reduced model based on modified EEFs will have fewer modes compared with the set of initial $\boldsymbol{N}$ EEFs-based models. The coefficients' matrix is derived from the nonlinear temporal dynamics of DPSs to introduce the information of higher modes to modified EEFs.

3.2. The Calculations of Coefficients' Matrix. Let $\boldsymbol{T}^{\boldsymbol{P}} = \{\boldsymbol{T}_1, \boldsymbol{T}_2, \cdots, \boldsymbol{T}_{\boldsymbol{r}_1}; \boldsymbol{T}_{\boldsymbol{i}}^T \boldsymbol{T}_{\boldsymbol{i}} = \boldsymbol{I}, \boldsymbol{i} = 1, \cdots, \boldsymbol{r}_1\}$ be a set of $\boldsymbol{r}_1$ orthogonal $\boldsymbol{N} \times \boldsymbol{N}$ matrices, where $\boldsymbol{r}_1$ denotes the number of matrices for excitation/perturbation directions. Let $\boldsymbol{M}^{\boldsymbol{s}_1} = \{\boldsymbol{c}_1, \boldsymbol{c}_2, \cdots, \boldsymbol{c}_{\boldsymbol{s}_1}; \boldsymbol{c}_{\boldsymbol{i}} > 0, \boldsymbol{i} = 1, \cdots, \boldsymbol{s}_1\}$ be a set of $\boldsymbol{s}_1$ positive constants, where $\boldsymbol{s}_1$ denotes the number of different excitation/perturbation sizes for each direction. Let $\boldsymbol{E}^{\boldsymbol{P}} = \{\boldsymbol{e}_1, \boldsymbol{e}_2, \cdots, \boldsymbol{e}_{\boldsymbol{p}}\}$ be $\boldsymbol{p}$ standard unit vectors in $\mathscr{R}^{\boldsymbol{p}}$, where $\boldsymbol{p}$ denotes the number of inputs. Given a function $\boldsymbol{x}(\boldsymbol{t})$, define the mean by

$$\langle \boldsymbol{x}(\boldsymbol{t}) \rangle = \lim_{\boldsymbol{T} \longrightarrow \infty} \frac{1}{\boldsymbol{T}} \int_0^{\boldsymbol{T}} \boldsymbol{x}(\boldsymbol{t})\, \boldsymbol{dt}. \tag{21}$$

The definitions of empirical controllability and observability matrices calculated according to the dynamical system (3) are given to compute the coefficients' matrix. The empirical controllability matrix [29–31] is defined by

$$\widehat{\boldsymbol{W}}_{\boldsymbol{C}} = \sum_{\boldsymbol{l}=1}^{\boldsymbol{r}_1} \sum_{\boldsymbol{m}=1}^{\boldsymbol{s}_1} \sum_{\boldsymbol{i}=1}^{\boldsymbol{p}} \frac{1}{\boldsymbol{r}_1 \cdot \boldsymbol{s}_1 \cdot \boldsymbol{c}_{\boldsymbol{m}}^2} \int_0^{\infty} \Phi^{\boldsymbol{ilm}}(\boldsymbol{t})\, \boldsymbol{dt}, \tag{22}$$

where $\Phi^{\boldsymbol{ilm}}(\boldsymbol{t}) \in \mathscr{R}^{N \times N}$ is given by

$$\Phi^{\boldsymbol{ilm}}(\boldsymbol{t}) = \left(\boldsymbol{x}^{\boldsymbol{ilm}}(\boldsymbol{t}) - \overline{\boldsymbol{x}}^{\boldsymbol{ilm}}\right)\left(\boldsymbol{x}^{\boldsymbol{ilm}}(\boldsymbol{t}) - \overline{\boldsymbol{x}}^{\boldsymbol{ilm}}\right)^T. \tag{23}$$

$\boldsymbol{x}^{\boldsymbol{ilm}}(\boldsymbol{t})$ and $\overline{\boldsymbol{x}}^{\boldsymbol{ilm}}$ are the state and mean state of $\boldsymbol{N}$ th dynamical system corresponding to the impulsive input $\boldsymbol{u}(\boldsymbol{t}) = \boldsymbol{c}_{\boldsymbol{m}} \boldsymbol{T}_{\boldsymbol{l}} \boldsymbol{e}_{\boldsymbol{i}} \delta(\boldsymbol{t})$, which is the system trajectory resulting from different excitations. The empirical controllability matrix $\widehat{\boldsymbol{W}}_{\boldsymbol{c}}$ has the property that its eigenvectors corresponding to nonzero eigenvalues span a subspace which contains the set of states reachable using the chosen initial impulsive inputs.

Let $\boldsymbol{T}^{\boldsymbol{N}} = \{\boldsymbol{T}_1, \boldsymbol{T}_2, \cdots, \boldsymbol{T}_{\boldsymbol{r}_2}; \boldsymbol{T}_{\boldsymbol{i}}^T \boldsymbol{T}_{\boldsymbol{i}} = \boldsymbol{I}, \boldsymbol{i} = 1, \cdots, \boldsymbol{r}_2\}$ be a set of $\boldsymbol{r}_2$ orthogonal $\boldsymbol{N} \times \boldsymbol{N}$ matrices, where $\boldsymbol{r}_2$ denotes the number of matrices for excitation/perturbation directions. Let $\boldsymbol{M}^{\boldsymbol{s}_2} = \{\boldsymbol{c}_1, \boldsymbol{c}_2, \cdots, \boldsymbol{c}_{\boldsymbol{s}_2}; \boldsymbol{c}_{\boldsymbol{i}} > 0, \boldsymbol{i} = 1, \cdots, \boldsymbol{s}_2\}$ be a set of $\boldsymbol{s}_2$ positive constants, where $\boldsymbol{s}_2$ denotes the number of different excitation/perturbation sizes for each direction. Let $\boldsymbol{E}^{\boldsymbol{N}} = \{\boldsymbol{e}_1, \boldsymbol{e}_2, \cdots, \boldsymbol{e}_{\boldsymbol{N}}\}$ be $\boldsymbol{N}$ standard unit vectors in $\mathscr{R}^{\boldsymbol{N}}$. The empirical observability matrix [29–31] is the analogue of the previous one for the output behaviors of the nonlinear system, which is defined by

$$\widehat{\boldsymbol{W}}_{\boldsymbol{O}} = \sum_{\boldsymbol{l}=1}^{\boldsymbol{r}_2} \sum_{\boldsymbol{m}=1}^{\boldsymbol{s}_2} \frac{1}{\boldsymbol{r}_2 \cdot \boldsymbol{s}_2 \cdot \boldsymbol{c}_{\boldsymbol{m}}^2} \int_0^{\infty} \boldsymbol{T}_{\boldsymbol{l}} \Psi^{\boldsymbol{lm}}(\boldsymbol{t})\, \boldsymbol{T}_{\boldsymbol{l}}^T \boldsymbol{dt} \tag{24}$$

where $\Psi^{\boldsymbol{lm}}(\boldsymbol{t}) \in \mathscr{R}^{N \times N}$ is given by

$$\Psi_{\boldsymbol{ij}}^{\boldsymbol{lm}}(\boldsymbol{t}) = \left(\boldsymbol{y}^{\boldsymbol{ilm}}(\boldsymbol{t}) - \overline{\boldsymbol{y}}^{\boldsymbol{ilm}}\right)^T \left(\boldsymbol{y}^{\boldsymbol{ilm}}(\boldsymbol{t}) - \overline{\boldsymbol{y}}^{\boldsymbol{ilm}}\right). \tag{25}$$

$\boldsymbol{y}^{\boldsymbol{ilm}}(\boldsymbol{t})$ and $\overline{\boldsymbol{y}}^{\boldsymbol{ilm}}$ are the output and mean output of $\boldsymbol{N}$ th dynamical system corresponding to the initial condition $\boldsymbol{x}_0 = \boldsymbol{c}_{\boldsymbol{m}} \boldsymbol{T}_{\boldsymbol{l}} \boldsymbol{e}_{\boldsymbol{l}}$ with $\boldsymbol{u}(\boldsymbol{t}) = 0$, which is the system trajectory resulting from different perturbations in the initial conditions with the steady inputs.

Each of the empirical matrices can be diagonalized by a linear coordinate transformation. This can be done for

an empirical matrix by determining the eigenvectors and corresponding eigenvalues of the matrix [29–31]. If the diagonalized ones of the matrices are equal, then the system is said to be in balanced form and the transformation is called a balancing transformation. The balancing-like transformation [30, 32] is used within a Galerkin projection in order to transform the matrices $\widehat{\boldsymbol{W}}_{\boldsymbol{C}}, \widehat{\boldsymbol{W}}_{\boldsymbol{O}}$ into the balanced form $\overline{\boldsymbol{W}}_{\boldsymbol{C}}, \overline{\boldsymbol{W}}_{\boldsymbol{O}}$. The calculations of transformation can be formulated as finding an invertible state transformation that makes two symmetric positive semidefinite matrices diagonal and equal in the states that are both controllable and observable. The proof that such a transformation exists is given by Zhou and Doyle [33]. The transformation $\overline{\boldsymbol{Q}}$ that diagonalizes the matrices and balances the states that are both observable and controllable is shown as follows:

$$\overline{\boldsymbol{Q}}\widehat{\boldsymbol{W}}_{\boldsymbol{C}}\overline{\boldsymbol{Q}}^{\boldsymbol{T}} = \left(\overline{\boldsymbol{Q}}^{-1}\right)^{\boldsymbol{T}}\widehat{\boldsymbol{W}}_{\boldsymbol{O}}\overline{\boldsymbol{Q}}^{-1} = \operatorname{diag}\left(\sigma_1, \sigma_2, \cdots, \sigma_N\right) \quad (26)$$

where $\overline{\boldsymbol{Q}}$ denotes the balanced transformation matrix, $\sigma_1 \geq \sigma_2 \geq \cdots \geq \sigma_N \geq 0$, and $\sigma_{\boldsymbol{i}}$'s are the Hankel singular values. The computations for the balanced transformation matrix $\overline{\boldsymbol{Q}}$ according to the matrices $\widehat{\boldsymbol{W}}_{\boldsymbol{C}}, \widehat{\boldsymbol{W}}_{\boldsymbol{O}}$ are given by Lall [30]. The state-coordinates of the nonlinear systems can be changed and truncated using the Galerkin projection. The row of $\overline{\boldsymbol{Q}}$ may be thought of as giving the 'modes' of the system associated with Hankel singular values. Thus, the coefficients matrix in (20) is set to be $\boldsymbol{Q} = \overline{\boldsymbol{Q}}(:, 1{:}\boldsymbol{k})^{\boldsymbol{T}}$ with the MATLAB style colon notation, which is the transposition of first $\boldsymbol{k}$ columns of transformation matrix $\overline{\boldsymbol{Q}}$.

3.3. Modified EEFs Based Model Reduction. The spatiotemporal variable of PDE (1) can be expanded onto the modified EEFs $\phi_{\boldsymbol{i}}(\boldsymbol{z})$ with corresponding temporal coefficients $\overline{\boldsymbol{x}}_{\boldsymbol{i}}(\boldsymbol{t})$ as follows:

$$\boldsymbol{X}(\boldsymbol{z}, \boldsymbol{t}) \approx \sum_{\boldsymbol{i}=1}^{\boldsymbol{k}} \overline{\boldsymbol{x}}_{\boldsymbol{i}}(\boldsymbol{t})\, \phi_{\boldsymbol{i}}(\boldsymbol{z}). \quad (27)$$

For (1), the following is derived:

$$\begin{aligned}
\sum_{\boldsymbol{i}=1}^{\boldsymbol{k}} \dot{\overline{\boldsymbol{x}}}_{\boldsymbol{i}}(\boldsymbol{t})\, \phi_{\boldsymbol{i}}(\boldsymbol{z}) &= \mathscr{A}\left(\sum_{\boldsymbol{i}=1}^{\boldsymbol{k}} \overline{\boldsymbol{x}}_{\boldsymbol{i}}(\boldsymbol{t})\, \phi_{\boldsymbol{i}}(\boldsymbol{z})\right) \\
&\quad + \mathscr{B}\left(\sum_{\boldsymbol{i}=1}^{\boldsymbol{m}} \boldsymbol{u}_{\boldsymbol{i}}(\boldsymbol{t})\, \boldsymbol{h}_{\boldsymbol{i}}(\boldsymbol{z})\right) + \mathscr{F}\left(\sum_{\boldsymbol{i}=1}^{\boldsymbol{k}} \overline{\boldsymbol{x}}_{\boldsymbol{i}}(\boldsymbol{t})\, \phi_{\boldsymbol{i}}(\boldsymbol{z}),\right. \\
&\quad \frac{\partial\left(\sum_{\boldsymbol{i}=1}^{\boldsymbol{k}} \overline{\boldsymbol{x}}_{\boldsymbol{i}}(\boldsymbol{t})\, \phi_{\boldsymbol{i}}(\boldsymbol{z})\right)}{\partial \boldsymbol{z}}, \cdots, \sum_{\boldsymbol{i}=1}^{\boldsymbol{m}} \boldsymbol{u}_{\boldsymbol{i}}(\boldsymbol{t})\, \boldsymbol{h}_{\boldsymbol{i}}(\boldsymbol{z}), \\
&\quad \left.\frac{\partial\left(\sum_{\boldsymbol{i}=1}^{\boldsymbol{m}} \boldsymbol{u}_{\boldsymbol{i}}(\boldsymbol{t})\, \boldsymbol{h}_{\boldsymbol{i}}(\boldsymbol{z})\right)}{\partial \boldsymbol{z}}, \cdots\right).
\end{aligned} \quad (28)$$

Using the Galerkin method, the following is then obtained:

$$\begin{aligned}
&\int_{\Omega} \sum_{\boldsymbol{i}=1}^{\boldsymbol{k}} \dot{\overline{\boldsymbol{x}}}_{\boldsymbol{i}}(\boldsymbol{t})\, \phi_{\boldsymbol{i}}(\boldsymbol{z})\, \phi_{\boldsymbol{j}}(\boldsymbol{z})\, \boldsymbol{dz} \\
&= \int_{\Omega} \left(\mathscr{A}\left(\sum_{\boldsymbol{i}=1}^{\boldsymbol{k}} \overline{\boldsymbol{x}}_{\boldsymbol{i}}(\boldsymbol{t})\, \phi_{\boldsymbol{i}}(\boldsymbol{z})\right)\right. \\
&\quad + \mathscr{B}\left(\sum_{\boldsymbol{i}=1}^{\boldsymbol{m}} \boldsymbol{u}_{\boldsymbol{i}}(\boldsymbol{t})\, \boldsymbol{h}_{\boldsymbol{i}}(\boldsymbol{z})\right)\Bigg) \phi_{\boldsymbol{j}}(\boldsymbol{z})\, \boldsymbol{dz} \\
&\quad + \int_{\Omega} \mathscr{F}\left(\sum_{\boldsymbol{i}=1}^{\boldsymbol{k}} \overline{\boldsymbol{x}}_{\boldsymbol{i}}(\boldsymbol{t})\, \phi_{\boldsymbol{i}}(\boldsymbol{z}), \frac{\partial\left(\sum_{\boldsymbol{i}=1}^{\boldsymbol{k}} \overline{\boldsymbol{x}}_{\boldsymbol{i}}(\boldsymbol{t})\, \phi_{\boldsymbol{i}}(\boldsymbol{z})\right)}{\partial \boldsymbol{z}}, \cdots,\right. \\
&\quad \left.\sum_{\boldsymbol{i}=1}^{\boldsymbol{m}} \boldsymbol{u}_{\boldsymbol{i}}(\boldsymbol{t})\, \boldsymbol{h}_{\boldsymbol{i}}(\boldsymbol{z}), \frac{\partial\left(\sum_{\boldsymbol{i}=1}^{\boldsymbol{m}} \boldsymbol{u}_{\boldsymbol{i}}(\boldsymbol{t})\, \boldsymbol{h}_{\boldsymbol{i}}(\boldsymbol{z})\right)}{\partial \boldsymbol{z}}, \cdots\right) \\
&\quad \cdot \phi_{\boldsymbol{j}}(\boldsymbol{z})\, \boldsymbol{dz}.
\end{aligned} \quad (29)$$

This will transform (29) into the following ODE system:

$$\begin{aligned}
\dot{\overline{\boldsymbol{x}}}(\boldsymbol{t}) &= \boldsymbol{D}^{-1}\overline{\boldsymbol{A}}\overline{\boldsymbol{x}}(\boldsymbol{t}) + \boldsymbol{D}^{-1}\overline{\boldsymbol{B}}\boldsymbol{u}(\boldsymbol{t}) + \boldsymbol{D}^{-1}\boldsymbol{g}\left(\overline{\boldsymbol{x}}(\boldsymbol{t}), \boldsymbol{u}(\boldsymbol{t})\right) \\
\boldsymbol{y}(\boldsymbol{t}) &= \overline{\boldsymbol{C}}\overline{\boldsymbol{x}}(\boldsymbol{t})
\end{aligned} \quad (30)$$

where the $\boldsymbol{D}^{-1}$ denotes the inverse matrix of $\boldsymbol{D}$,

$$\begin{aligned}
&\overline{\boldsymbol{x}}(\boldsymbol{t}) = \left[\overline{\boldsymbol{x}}_1(\boldsymbol{t}), \overline{\boldsymbol{x}}_2(\boldsymbol{t}), \cdots, \overline{\boldsymbol{x}}_{\boldsymbol{k}}(\boldsymbol{t})\right]^{\boldsymbol{T}}, \\
&\boldsymbol{u}(\boldsymbol{t}) = \left[\boldsymbol{u}_1(\boldsymbol{t}), \boldsymbol{u}_2(\boldsymbol{t}), \cdots, \boldsymbol{u}_{\boldsymbol{m}}(\boldsymbol{t})\right]^{\boldsymbol{T}}, \\
&\boldsymbol{g}\left(\overline{\boldsymbol{x}}(\boldsymbol{t}), \boldsymbol{u}(\boldsymbol{t})\right) = \left[\boldsymbol{g}_1\left(\overline{\boldsymbol{x}}(\boldsymbol{t}), \boldsymbol{u}(\boldsymbol{t})\right), \cdots, \boldsymbol{g}_{\boldsymbol{k}}\left(\overline{\boldsymbol{x}}(\boldsymbol{t}),\right.\right. \\
&\quad \left.\left.\boldsymbol{u}(\boldsymbol{t})\right)\right]^{\boldsymbol{T}}, \\
&\boldsymbol{g}_{\boldsymbol{i}}\left(\overline{\boldsymbol{x}}(\boldsymbol{t}), \boldsymbol{u}(\boldsymbol{t})\right) = \int_{\Omega} \mathscr{F}\left(\sum_{\boldsymbol{i}=1}^{\boldsymbol{k}} \overline{\boldsymbol{x}}_{\boldsymbol{i}}(\boldsymbol{t})\, \phi_{\boldsymbol{i}}(\boldsymbol{z}),\right. \\
&\quad \frac{\partial\left(\sum_{\boldsymbol{i}=1}^{\boldsymbol{k}} \overline{\boldsymbol{x}}_{\boldsymbol{i}}(\boldsymbol{t})\, \phi_{\boldsymbol{i}}(\boldsymbol{z})\right)}{\partial \boldsymbol{z}}, \cdots, \sum_{\boldsymbol{i}=1}^{\boldsymbol{m}} \boldsymbol{u}_{\boldsymbol{i}}(\boldsymbol{t})\, \boldsymbol{h}_{\boldsymbol{i}}(\boldsymbol{z}), \\
&\quad \left.\frac{\partial\left(\sum_{\boldsymbol{i}=1}^{\boldsymbol{m}} \boldsymbol{u}_{\boldsymbol{i}}(\boldsymbol{t})\, \boldsymbol{h}_{\boldsymbol{i}}(\boldsymbol{z})\right)}{\partial \boldsymbol{z}}, \cdots\right) \phi_{\boldsymbol{j}}(\boldsymbol{z})\, \boldsymbol{dz}.
\end{aligned} \quad (31)$$

Letting $\boldsymbol{Q}_{\boldsymbol{i}}$ denotes the $\boldsymbol{i}$ th row of the coefficient matrix $\boldsymbol{Q}$, then the elements of matrices $\boldsymbol{D}, \boldsymbol{A}, \boldsymbol{B}, \boldsymbol{C}$ can be calculated as follows:

$$\begin{aligned}
\boldsymbol{D}_{\boldsymbol{ij}} &= \int_{\Omega} \phi_{\boldsymbol{i}}(\boldsymbol{z})\, \phi_{\boldsymbol{j}}(\boldsymbol{z})\, \boldsymbol{dz} \\
&= \sum_{\boldsymbol{l}=1}^{\boldsymbol{N}} \boldsymbol{Q}_{\boldsymbol{il}}\boldsymbol{Q}_{\boldsymbol{jl}} \int_{\Omega} \varphi_{\boldsymbol{i}}(\boldsymbol{z})\, \varphi_{\boldsymbol{j}}(\boldsymbol{z})\, \boldsymbol{dz} = \boldsymbol{Q}_{\boldsymbol{i}}\boldsymbol{Q}_{\boldsymbol{j}}^{\boldsymbol{T}}, \\
\overline{\boldsymbol{A}}_{\boldsymbol{ij}} &= \int_{\Omega} \mathscr{A}\left(\phi_{\boldsymbol{j}}(\boldsymbol{z})\right) \phi_{\boldsymbol{i}}(\boldsymbol{z})\, \boldsymbol{dz} \\
&= \int_{\Omega} \mathscr{A}\left(\sum_{\boldsymbol{l}=1}^{\boldsymbol{N}} \boldsymbol{Q}_{\boldsymbol{jl}}\varphi_{\boldsymbol{l}}(\boldsymbol{z})\right)\left(\sum_{\boldsymbol{l}=1}^{\boldsymbol{N}} \boldsymbol{Q}_{\boldsymbol{il}}\varphi_{\boldsymbol{l}}(\boldsymbol{z})\right) \boldsymbol{dz} \\
&= \boldsymbol{Q}_{\boldsymbol{i}}\boldsymbol{A}\boldsymbol{Q}_{\boldsymbol{j}}^{\boldsymbol{T}},
\end{aligned}$$

$$\begin{aligned}\overline{\boldsymbol{B}}_{ij} &= \int_{\Omega} \mathscr{B}\left(\boldsymbol{h}_j(\boldsymbol{z})\right)\phi_i(\boldsymbol{z})\,d\boldsymbol{z} \\ &= \int_{\Omega} \mathscr{B}\left(\boldsymbol{h}_j(\boldsymbol{z})\right)\left(\sum_{l=1}^{N}\boldsymbol{Q}_{il}\varphi_l(\boldsymbol{z})\right)d\boldsymbol{z} = \boldsymbol{Q}_i\boldsymbol{B}_j, \\ \overline{\boldsymbol{C}}_{ij} &= \phi_j(\boldsymbol{z}_i) = [\boldsymbol{S}_{i1}\ \ \boldsymbol{S}_{i2}\ \ \cdots\ \ \boldsymbol{S}_{iN}]\,\boldsymbol{Q}_j^T.\end{aligned} \tag{32}$$

For simplicity, the equation can be derived as

$$\begin{aligned}\dot{\overline{\boldsymbol{x}}}(\boldsymbol{t}) &= \boldsymbol{A}_l\overline{\boldsymbol{x}}(\boldsymbol{t}) + \boldsymbol{B}_l\boldsymbol{u}(\boldsymbol{t}) + \overline{\boldsymbol{f}}\left(\overline{\boldsymbol{x}}(\boldsymbol{t}), \boldsymbol{u}(\boldsymbol{t})\right) \\ \boldsymbol{y}(\boldsymbol{t}) &= \boldsymbol{C}_l\overline{\boldsymbol{x}}(\boldsymbol{t})\end{aligned} \tag{33}$$

where $\boldsymbol{A}_l = \boldsymbol{D}^{-1}\overline{\boldsymbol{A}}$, $\boldsymbol{B}_l = \boldsymbol{D}^{-1}\overline{\boldsymbol{B}}$, and $\boldsymbol{C}_l = \overline{\boldsymbol{C}}$,

$$\overline{\boldsymbol{f}}\left(\overline{\boldsymbol{x}}(\boldsymbol{t}), \boldsymbol{u}(\boldsymbol{t})\right) = \boldsymbol{D}^{-1}\boldsymbol{g}\left(\overline{\boldsymbol{x}}(\boldsymbol{t}), \boldsymbol{u}(\boldsymbol{t})\right). \tag{34}$$

3.4. Model Reduction Performances. The effectiveness of the improved EEFs in our previous work was proofed in [28], and model reduction performance of modified EEFs can be given in a similar way. Suppose that there are enough sensors for measurements and $\boldsymbol{Y}_{\boldsymbol{P}}(\boldsymbol{z}, \boldsymbol{t})$ denotes the predicted spatiotemporal variable for $\boldsymbol{X}(\boldsymbol{z}, \boldsymbol{t})$. Let $\boldsymbol{Y}_j = [\boldsymbol{Y}(\boldsymbol{z}_1, \boldsymbol{t}_j), \boldsymbol{Y}(\boldsymbol{z}_2, \boldsymbol{t}_j), \cdots, \boldsymbol{Y}(\boldsymbol{z}_M, \boldsymbol{t}_j)]^T$ and $\boldsymbol{Y}_{\boldsymbol{P}j} = [\boldsymbol{Y}_{\boldsymbol{P}}(\boldsymbol{z}_1, \boldsymbol{t}_j), \boldsymbol{Y}_{\boldsymbol{P}}(\boldsymbol{z}_2, \boldsymbol{t}_j), \cdots, \boldsymbol{Y}_{\boldsymbol{P}}(\boldsymbol{z}_M, \boldsymbol{t}_j)]^T$ be the measured data of spatiotemporal variable $\boldsymbol{Y}(\boldsymbol{z}, \boldsymbol{t})$ and $\boldsymbol{Y}_{\boldsymbol{P}}(\boldsymbol{z}, \boldsymbol{t})$ at $\boldsymbol{M}$ spatial locations $\boldsymbol{z}_1, \boldsymbol{z}_2, \cdots, \boldsymbol{z}_M$ and the sampling times $\boldsymbol{t}_j$, respectively. To evaluate the model reduction performance at any sampling time $\boldsymbol{t}_j$ by using modified EEFs and initial EEFs, the root-square error (RSE) as a performance index is introduced for comparisons

$$\boldsymbol{RSE} = \sqrt{\sum_{l=1}^{M}\boldsymbol{e}\left(\boldsymbol{z}_i, \boldsymbol{t}_j\right)^2}, \tag{35}$$

where $\boldsymbol{e}(\boldsymbol{z}_l, \boldsymbol{t}_j) = \boldsymbol{Y}(\boldsymbol{z}_l, \boldsymbol{t}_j) - \boldsymbol{Y}_{\boldsymbol{P}}(\boldsymbol{z}_l, \boldsymbol{t}_j)$. The effectiveness of model reduction with the modified EEFs is given in the following theorem.

Theorem 1. *Given an coefficient matrix $\boldsymbol{Q}$ obtained in Section 3.2, then the RSE based on $\boldsymbol{k}$ modified EEFs is smaller than that based on $\boldsymbol{k}$ initial EEFs at any sampling time $\boldsymbol{t}_j$ if $\boldsymbol{E}(\boldsymbol{Q}\boldsymbol{Q}^T)^{-1}\boldsymbol{Q}\boldsymbol{E}_1\boldsymbol{E}_2\boldsymbol{Q}^T(\boldsymbol{Q}\boldsymbol{Q}^T)^{-1}\ \boldsymbol{E}$ is negative semidefinite, where $\boldsymbol{E}$ is a diagonal matrix with $\boldsymbol{E}_{ii} = \boldsymbol{Q}_i\boldsymbol{Q}_i^T$, $\boldsymbol{i} = 1, 2, \cdots, \boldsymbol{k}$, and*

$$\begin{aligned}\boldsymbol{E}_1 &= \begin{pmatrix}\boldsymbol{I}_k & 0 \\ 0 & 0_{\boldsymbol{N}-\boldsymbol{k}}\end{pmatrix} - \boldsymbol{Q}^T\boldsymbol{E}^{-1}\boldsymbol{Q}, \\ \boldsymbol{E}_2 &= \begin{pmatrix}\boldsymbol{I}_k & 0 \\ 0 & 2\boldsymbol{I}_{\boldsymbol{N}-\boldsymbol{k}}\end{pmatrix} - \boldsymbol{Q}^T\boldsymbol{E}^{-1}\boldsymbol{Q}.\end{aligned} \tag{36}$$

Proof. From POD decomposition for the measured spatiotemporal observation at the sampling time $\boldsymbol{t}_j$, we have

$$\boldsymbol{Y}_j = \overline{\boldsymbol{Y}} + \sum_{i=1}^{N}\boldsymbol{y}_i\left(\boldsymbol{t}_j\right)\varphi_i. \tag{37}$$

The predicted output based on $\boldsymbol{k}$ initial EEFs at the sampling time t_j is as follows:

$$\boldsymbol{Y}_{\boldsymbol{IE}j} = \overline{\boldsymbol{Y}} + \sum_{i=1}^{k}\boldsymbol{y}_i\left(\boldsymbol{t}_j\right)\varphi_i. \tag{38}$$

The predicted output based on $\boldsymbol{k}$ modified EEFs at sampling time $\boldsymbol{t}_j$ can be expressed as follows:

$$\boldsymbol{Y}_{\boldsymbol{EE}j} = \overline{\boldsymbol{Y}} + \sum_{i=1}^{k}\overline{\boldsymbol{y}}_i\left(\boldsymbol{t}_j\right)\phi_i. \tag{39}$$

The RSE with $\boldsymbol{k}$ initial EEFs is defined as

$$\boldsymbol{G}_{\boldsymbol{IE}}\left(\boldsymbol{t}_j\right) = \sqrt{\sum_{l=1}^{M}\left(\sum_{i=k+1}^{N}\boldsymbol{y}_i\left(\boldsymbol{t}_j\right)\varphi_i\left(\boldsymbol{z}_l\right)\right)^2}. \tag{40}$$

The RSE with $\boldsymbol{k}$ modified EEFs is defined as

$$\begin{aligned}&\boldsymbol{G}_{\boldsymbol{EE}}\left(\boldsymbol{t}_j\right) \\ &= \sqrt{\sum_{l=1}^{M}\left(\sum_{i=1}^{N}\boldsymbol{y}_i\left(\boldsymbol{t}_j\right)\varphi_i\left(\boldsymbol{z}_l\right) - \sum_{i=1}^{k}\overline{\boldsymbol{y}}_i\left(\boldsymbol{t}_j\right)\phi_i\left(\boldsymbol{z}_l\right)\right)^2}.\end{aligned} \tag{41}$$

To prove that $0 \le \boldsymbol{G}_{\boldsymbol{EE}}(\boldsymbol{t}_j) < \boldsymbol{G}_{\boldsymbol{IE}}(\boldsymbol{t}_j)$, only the following inequality has to be proved:

$$\left(\boldsymbol{G}_{\boldsymbol{EE}}\left(\boldsymbol{t}_j\right)\right)^2 < \left(\boldsymbol{G}_{\boldsymbol{IE}}\left(\boldsymbol{t}_j\right)\right)^2. \tag{42}$$

Substituting (40) and (41) into (42) yields

$$\begin{aligned}&\sum_{l=1}^{M}\left(\sum_{i=1}^{N}\boldsymbol{y}_i\left(\boldsymbol{t}_j\right)\varphi_i\left(\boldsymbol{z}_l\right) - \sum_{i=1}^{k}\overline{\boldsymbol{y}}_i\left(\boldsymbol{t}_j\right)\phi_i\left(\boldsymbol{z}_l\right)\right)^2 \\ &< \sum_{l=1}^{M}\left(\sum_{i=k+1}^{N}\boldsymbol{y}_i\left(\boldsymbol{t}_j\right)\varphi_i\left(\boldsymbol{z}_l\right)\right)^2.\end{aligned} \tag{43}$$

Then, we have

$$\begin{aligned}&\sum_{l=1}^{M}\left(\left(\sum_{i=1}^{N}\boldsymbol{y}_i\left(\boldsymbol{t}_j\right)\varphi_i\left(\boldsymbol{z}_l\right) - \sum_{i=1}^{k}\overline{\boldsymbol{y}}_i\left(\boldsymbol{t}_j\right)\phi_i\left(\boldsymbol{z}_l\right)\right)^2\right. \\ &\left. - \left(\sum_{i=k+1}^{N}\boldsymbol{y}_i\left(\boldsymbol{t}_j\right)\varphi_i\left(\boldsymbol{z}_l\right)\right)^2\right) < 0.\end{aligned} \tag{44}$$

And the following inequality can be derived:

$$\begin{aligned}&\sum_{l=1}^{M}\left\{\left(\sum_{i=1}^{k}\boldsymbol{y}_i\left(\boldsymbol{t}_j\right)\varphi_i\left(\boldsymbol{z}_l\right) - \sum_{i=1}^{k}\overline{\boldsymbol{y}}_i\left(\boldsymbol{t}_j\right)\phi_i\left(\boldsymbol{z}_l\right)\right)\right. \\ &\cdot\left(\sum_{i=k+1}^{N}\boldsymbol{y}_i\left(\boldsymbol{t}_j\right)\varphi_i\left(\boldsymbol{z}_l\right) + \sum_{i=1}^{N}\boldsymbol{y}_i\left(\boldsymbol{t}_j\right)\varphi_i\left(\boldsymbol{z}_l\right)\right. \\ &\left.\left. - \sum_{i=1}^{k}\overline{\boldsymbol{y}}_i\left(\boldsymbol{t}_j\right)\phi_i\left(\boldsymbol{z}_l\right)\right)\right\} < 0.\end{aligned} \tag{45}$$

Note that

$$\overline{\boldsymbol{y}}_{\boldsymbol{i}}\left(\boldsymbol{t}_{\boldsymbol{j}}\right)=\frac{\left(\boldsymbol{Y}\left(\boldsymbol{z},\boldsymbol{t}\right)-\overline{\boldsymbol{Y}},\boldsymbol{\phi}_{\boldsymbol{i}}\right)}{\left(\boldsymbol{\phi}_{\boldsymbol{i}},\boldsymbol{\phi}_{\boldsymbol{i}}\right)} \tag{46}$$

where $(\boldsymbol{\phi}_{\boldsymbol{i}},\boldsymbol{\phi}_{\boldsymbol{i}})=(\sum_{\boldsymbol{j}=1}^{\boldsymbol{N}}\boldsymbol{Q}_{\boldsymbol{ij}}\boldsymbol{\varphi}_{\boldsymbol{j}},\sum_{\boldsymbol{j}=1}^{\boldsymbol{N}}\boldsymbol{Q}_{\boldsymbol{ij}}\boldsymbol{\varphi}_{\boldsymbol{j}})=\boldsymbol{Q}_{\boldsymbol{i}}\boldsymbol{Q}_{\boldsymbol{i}}^{\boldsymbol{T}}$,

$$\begin{aligned}\left(\boldsymbol{Y}\left(\boldsymbol{z},\boldsymbol{t}\right)-\overline{\boldsymbol{Y}},\boldsymbol{\phi}_{\boldsymbol{i}}\right)&=\left(\boldsymbol{Y}\left(\boldsymbol{z},\boldsymbol{t}\right)-\overline{\boldsymbol{Y}},\sum_{\boldsymbol{j}=1}^{\boldsymbol{N}}\boldsymbol{Q}_{\boldsymbol{ij}}\boldsymbol{\varphi}_{\boldsymbol{j}}\right)\\&=\left[\boldsymbol{y}_1\left(\boldsymbol{t}\right),\cdots,\boldsymbol{y}_{\boldsymbol{N}}\left(\boldsymbol{t}\right)\right]\begin{bmatrix}\boldsymbol{Q}_{1\boldsymbol{i}}\\\vdots\\\boldsymbol{Q}_{\boldsymbol{Ni}}\end{bmatrix}.\end{aligned} \tag{47}$$

Let $\boldsymbol{E}_{\boldsymbol{k}\times\boldsymbol{k}}$ be the diagonal matrix and $\boldsymbol{E}_{\boldsymbol{ii}}=\boldsymbol{Q}_{\boldsymbol{i}}\boldsymbol{Q}_{\boldsymbol{i}}^{\boldsymbol{T}}$, $\boldsymbol{i}=1,2,\cdots,\boldsymbol{k}$; then

$$\left[\overline{\boldsymbol{y}}_1\left(\boldsymbol{t}\right),\cdots,\overline{\boldsymbol{y}}_{\boldsymbol{k}}\left(\boldsymbol{t}\right)\right]=\left[\boldsymbol{y}_1\left(\boldsymbol{t}\right),\cdots,\boldsymbol{y}_{\boldsymbol{N}}\left(\boldsymbol{t}\right)\right]\boldsymbol{Q}^{\boldsymbol{T}}\boldsymbol{E}^{-1} \tag{48}$$

Then

$$\begin{aligned}&\left[\boldsymbol{y}_1\left(\boldsymbol{t}\right),\cdots,\boldsymbol{y}_{\boldsymbol{N}}\left(\boldsymbol{t}\right)\right]\\&=\left[\overline{\boldsymbol{y}}_1\left(\boldsymbol{t}\right),\cdots,\overline{\boldsymbol{y}}_{\boldsymbol{k}}\left(\boldsymbol{t}\right)\right]\boldsymbol{E}\left(\boldsymbol{Q}\boldsymbol{Q}^{\boldsymbol{T}}\right)^{-1}\boldsymbol{Q}\end{aligned} \tag{49}$$

In inequality (45),

$$\begin{aligned}&\left(\sum_{\boldsymbol{i}=1}^{\boldsymbol{k}}\boldsymbol{y}_{\boldsymbol{i}}\left(\boldsymbol{t}_{\boldsymbol{j}}\right)\boldsymbol{\varphi}_{\boldsymbol{i}}\left(\boldsymbol{z}_{\boldsymbol{l}}\right)-\sum_{\boldsymbol{i}=1}^{\boldsymbol{k}}\overline{\boldsymbol{y}}_{\boldsymbol{i}}\left(\boldsymbol{t}_{\boldsymbol{j}}\right)\boldsymbol{\phi}_{\boldsymbol{i}}\left(\boldsymbol{z}_{\boldsymbol{l}}\right)\right)\\&=\left(\boldsymbol{\varphi}_1\left(\boldsymbol{z}_{\boldsymbol{l}}\right),\boldsymbol{\varphi}_2\left(\boldsymbol{z}_{\boldsymbol{l}}\right),\cdots,\boldsymbol{\varphi}_{\boldsymbol{N}}\left(\boldsymbol{z}_{\boldsymbol{l}}\right)\right)\\&\cdot\boldsymbol{E}_1\begin{pmatrix}\boldsymbol{y}_1\left(\boldsymbol{t}_{\boldsymbol{j}}\right)\\\boldsymbol{y}_2\left(\boldsymbol{t}_{\boldsymbol{j}}\right)\\\vdots\\\boldsymbol{y}_{\boldsymbol{N}}\left(\boldsymbol{t}_{\boldsymbol{j}}\right)\end{pmatrix},\end{aligned} \tag{50}$$

$$\begin{aligned}&\left(\sum_{\boldsymbol{i}=\boldsymbol{k}+1}^{\boldsymbol{N}}\boldsymbol{y}_{\boldsymbol{i}}\left(\boldsymbol{t}_{\boldsymbol{j}}\right)\boldsymbol{\varphi}_{\boldsymbol{i}}\left(\boldsymbol{z}_{\boldsymbol{l}}\right)+\sum_{\boldsymbol{i}=1}^{\boldsymbol{N}}\boldsymbol{y}_{\boldsymbol{i}}\left(\boldsymbol{t}_{\boldsymbol{j}}\right)\boldsymbol{\varphi}_{\boldsymbol{i}}\left(\boldsymbol{z}_{\boldsymbol{l}}\right)\right.\\&\left.-\sum_{\boldsymbol{i}=1}^{\boldsymbol{k}}\overline{\boldsymbol{y}}_{\boldsymbol{i}}\left(\boldsymbol{t}_{\boldsymbol{j}}\right)\boldsymbol{\phi}_{\boldsymbol{i}}\left(\boldsymbol{z}_{\boldsymbol{l}}\right)\right)\\&=\left(\boldsymbol{\varphi}_1\left(\boldsymbol{z}_{\boldsymbol{l}}\right),\boldsymbol{\varphi}_2\left(\boldsymbol{z}_{\boldsymbol{l}}\right),\cdots,\boldsymbol{\varphi}_{\boldsymbol{N}}\left(\boldsymbol{z}_{\boldsymbol{l}}\right)\right)\\&\cdot\boldsymbol{E}_2\begin{pmatrix}\boldsymbol{y}_1\left(\boldsymbol{t}_{\boldsymbol{j}}\right)\\\boldsymbol{y}_2\left(\boldsymbol{t}_{\boldsymbol{j}}\right)\\\vdots\\\boldsymbol{y}_{\boldsymbol{N}}\left(\boldsymbol{t}_{\boldsymbol{j}}\right)\end{pmatrix},\end{aligned} \tag{51}$$

where

$$\begin{aligned}\boldsymbol{E}_1&=\begin{pmatrix}\boldsymbol{I}_{\boldsymbol{k}}&0\\0&0_{\boldsymbol{N}-\boldsymbol{k}}\end{pmatrix}-\boldsymbol{Q}^{\boldsymbol{T}}\boldsymbol{E}^{-1}\boldsymbol{Q},\\\boldsymbol{E}_2&=\begin{pmatrix}\boldsymbol{I}_{\boldsymbol{k}}&0\\0&2\boldsymbol{I}_{\boldsymbol{N}-\boldsymbol{k}}\end{pmatrix}-\boldsymbol{Q}^{\boldsymbol{T}}\boldsymbol{E}^{-1}\boldsymbol{Q}.\end{aligned} \tag{52}$$

Then (50) timing (51) yields

$$\begin{aligned}&\left(\boldsymbol{G}_{\boldsymbol{EE}}\left(\boldsymbol{t}_{\boldsymbol{j}}\right)\right)^2-\left(\boldsymbol{G}_{\boldsymbol{IE}}\left(\boldsymbol{t}_{\boldsymbol{j}}\right)\right)^2\\&=\left(\boldsymbol{y}_1\left(\boldsymbol{t}_{\boldsymbol{j}}\right),\boldsymbol{y}_2\left(\boldsymbol{t}_{\boldsymbol{j}}\right),\cdots,\boldsymbol{y}_{\boldsymbol{N}}\left(\boldsymbol{t}_{\boldsymbol{j}}\right)\right)\\&\cdot\boldsymbol{E}_1\boldsymbol{E}_3\boldsymbol{E}_2\begin{pmatrix}\boldsymbol{y}_1\left(\boldsymbol{t}_{\boldsymbol{j}}\right)\\\boldsymbol{y}_2\left(\boldsymbol{t}_{\boldsymbol{j}}\right)\\\vdots\\\boldsymbol{y}_{\boldsymbol{N}}\left(\boldsymbol{t}_{\boldsymbol{j}}\right)\end{pmatrix}.\end{aligned} \tag{53}$$

where

$$\boldsymbol{E}_3=\begin{bmatrix}\sum_{\boldsymbol{l}=1}^{\boldsymbol{M}}\boldsymbol{\varphi}_1^{\boldsymbol{T}}\left(\boldsymbol{z}_{\boldsymbol{l}}\right)\boldsymbol{\varphi}_1\left(\boldsymbol{z}_{\boldsymbol{l}}\right)&\cdots&\sum_{\boldsymbol{l}=1}^{\boldsymbol{M}}\boldsymbol{\varphi}_1^{\boldsymbol{T}}\left(\boldsymbol{z}_{\boldsymbol{l}}\right)\boldsymbol{\varphi}_{\boldsymbol{N}}\left(\boldsymbol{z}_{\boldsymbol{l}}\right)\\\vdots&\cdots&\vdots\\\sum_{\boldsymbol{l}=1}^{\boldsymbol{M}}\boldsymbol{\varphi}_{\boldsymbol{N}}^{\boldsymbol{T}}\left(\boldsymbol{z}_{\boldsymbol{l}}\right)\boldsymbol{\varphi}_1\left(\boldsymbol{z}_{\boldsymbol{l}}\right)&\cdots&\sum_{\boldsymbol{l}=1}^{\boldsymbol{M}}\boldsymbol{\varphi}_{\boldsymbol{N}}^{\boldsymbol{T}}\left(\boldsymbol{z}_{\boldsymbol{l}}\right)\boldsymbol{\varphi}_{\boldsymbol{N}}\left(\boldsymbol{z}_{\boldsymbol{l}}\right)\end{bmatrix}. \tag{54}$$

As $(\boldsymbol{\varphi}_1,\boldsymbol{\varphi}_2,\cdots,\boldsymbol{\varphi}_{\boldsymbol{N}})$ are orthogonal each other, thus

$$\boldsymbol{E}_3=\begin{bmatrix}1&0&\cdots&0\\0&1&\cdots&0\\\vdots&\vdots&\ddots&\vdots\\0&0&0&1\end{bmatrix}=\boldsymbol{I}_{\boldsymbol{N}} \tag{55}$$

Substituting (55) and (49) into (53) yields

$$\begin{aligned}&\left(\boldsymbol{G}_{\boldsymbol{EE}}\left(\boldsymbol{t}_{\boldsymbol{j}}\right)\right)^2-\left(\boldsymbol{G}_{\boldsymbol{IE}}\left(\boldsymbol{t}_{\boldsymbol{j}}\right)\right)^2\\&=\left(\overline{\boldsymbol{y}}_1\left(\boldsymbol{t}_{\boldsymbol{j}}\right),\overline{\boldsymbol{y}}_2\left(\boldsymbol{t}_{\boldsymbol{j}}\right),\cdots,\overline{\boldsymbol{y}}_{\boldsymbol{k}}\left(\boldsymbol{t}_{\boldsymbol{j}}\right)\right)\cdot\boldsymbol{E}\left(\boldsymbol{Q}\boldsymbol{Q}^{\boldsymbol{T}}\right)^{-1}\\&\cdot\boldsymbol{Q}\boldsymbol{E}_1\boldsymbol{E}_2\boldsymbol{Q}^{\boldsymbol{T}}\left(\boldsymbol{Q}\boldsymbol{Q}^{\boldsymbol{T}}\right)^{-1}\boldsymbol{E}\begin{pmatrix}\overline{\boldsymbol{y}}_1\left(\boldsymbol{t}_{\boldsymbol{j}}\right)\\\overline{\boldsymbol{y}}_2\left(\boldsymbol{t}_{\boldsymbol{j}}\right)\\\vdots\\\overline{\boldsymbol{y}}_{\boldsymbol{k}}\left(\boldsymbol{t}_{\boldsymbol{j}}\right)\end{pmatrix}\end{aligned} \tag{56}$$

If $\boldsymbol{E}(\boldsymbol{Q}\boldsymbol{Q}^{\boldsymbol{T}})^{-1}\boldsymbol{Q}\boldsymbol{E}_1\boldsymbol{E}_2\boldsymbol{Q}^{\boldsymbol{T}}(\boldsymbol{Q}\boldsymbol{Q}^{\boldsymbol{T}})^{-1}\boldsymbol{E}$ is negative semi-definite, then $\boldsymbol{G}_{\boldsymbol{EE}}(\boldsymbol{t}_{\boldsymbol{j}})<\boldsymbol{G}_{\boldsymbol{IE}}(\boldsymbol{t}_{\boldsymbol{j}})$ because of $\boldsymbol{G}_{\boldsymbol{IE}}(\boldsymbol{t}_{\boldsymbol{j}})\geq 0$ and $\boldsymbol{G}_{\boldsymbol{EE}}(\boldsymbol{t}_{\boldsymbol{j}})\geq 0$. This completes the proof and the results will be used in the numerical example. This theorem can only certificate that the modified EEFs is superior to the initial EEFs under certain constrained conditions. The comparisons for the performances of modified EEFs and improved EEFs [28] are given in the numerical example. □

4. Modified EEFs-Based Neural Modelling

Let $\boldsymbol{y} = \{\boldsymbol{y}_i(\boldsymbol{t}_j)\}_{i=1,j=1}^{N,L}$ be the corresponding temporal coefficients of initial EEFs for the measured output $\boldsymbol{Y} = \{\boldsymbol{Y}(\boldsymbol{z}_i, \boldsymbol{t}_j)\}_{i=1,j=1}^{M,L}$. The corresponding temporal coefficients of modified EEFs can be derived as follows:

$$(\boldsymbol{Y}, \phi_i) = \left(\boldsymbol{Y}, \sum_{p=1}^{N} \boldsymbol{Q}_{ip}\varphi_p\right) = \boldsymbol{Q}_i \boldsymbol{y} \tag{57}$$

where $\boldsymbol{Q}_i$ denotes the $\boldsymbol{i}$ th row of coefficient matrix. The corresponding temporal coefficients $\widetilde{\boldsymbol{y}} = \{\overline{\boldsymbol{y}}_i(\boldsymbol{t}_j)\}_{i=1,j=1}^{k,L}$ can also be derived as follows:

$$\widetilde{\boldsymbol{y}}_{k\times L} = \boldsymbol{Q}_{k\times N} \cdot \boldsymbol{y}_{N\times L}. \tag{58}$$

In the Galerkin method, obtaining an exact analytical description of the ODE systems is difficult and complex because of the nonlinearities in the inner product. Therefore, the neural networks can be used to identify the long-term dynamical behaviors from the input $\boldsymbol{u}(\boldsymbol{t})$ and the corresponding temporal coefficients $\widetilde{\boldsymbol{y}}$ of modified EEFs

$$\widehat{\boldsymbol{y}}(\boldsymbol{p}+1) = \boldsymbol{NN}(\widehat{\boldsymbol{y}}(\boldsymbol{p}), \boldsymbol{u}(\boldsymbol{p})), \tag{59}$$

where $\widehat{\boldsymbol{y}}(\boldsymbol{p}) = [\widehat{\boldsymbol{y}}_1(\boldsymbol{p}), \widehat{\boldsymbol{y}}_2(\boldsymbol{p}), \cdots, \widehat{\boldsymbol{y}}_{\boldsymbol{k}}(\boldsymbol{p})]^T$, $\boldsymbol{k} < \boldsymbol{N}$.

The advantage of the neural networks is its ability to model complex nonlinear relationships without any assumptions on the nature of these relationships. The most often used neural networks include the radial basis function networks (RBF), backpropagation (BP) neural networks [28], among others. The present study employs a feedforward BP neural network to construct low-dimensional substitute model for the dynamics of DPSs. The prediction output of nonlinear DPSs is obtained by synthesis of temporal predicted outputs and the modified EEFs

$$\boldsymbol{Y}_p(\boldsymbol{z}, \boldsymbol{p}) = \overline{\boldsymbol{Y}} + \sum_{i=1}^{k} \widehat{\boldsymbol{y}}_i(\boldsymbol{p})\, \phi_i(\boldsymbol{z}). \tag{60}$$

5. A Numerical Example

Suppose that $\boldsymbol{Y}(\boldsymbol{z}, \boldsymbol{t})$ and $\boldsymbol{Y}_p(\boldsymbol{z}, \boldsymbol{t})$ are the measured and predicted outputs at the M spatial locations $\boldsymbol{z}_1, \boldsymbol{z}_2, \cdots, \boldsymbol{z}_M$ and sampling times $\boldsymbol{t}_1, \boldsymbol{t}_2, \cdots, \boldsymbol{t}_L$, respectively. For an easy comparison, the root of mean squared error (RMSE) is set up as the performance index as follows:

$$\boldsymbol{RMSE} = \sqrt{\frac{\sum_{i=1}^{M}\sum_{j=1}^{L}\left(\boldsymbol{e}\left(\boldsymbol{z}_i, \boldsymbol{t}_j\right)\right)^2}{\boldsymbol{ML}}} \tag{61}$$

where $\boldsymbol{e}(\boldsymbol{z}_i, \boldsymbol{t}_j) = \boldsymbol{Y}(\boldsymbol{z}_i, \boldsymbol{t}_j) - \boldsymbol{Y}_p(\boldsymbol{z}_i, \boldsymbol{t}_j)$.

To evaluate the performance of modified EEFs for model reduction, the rescaled Kuramoto-sivashinsky (K-S) equation [34, 35] in one-space dimension is considered. The K-S equations are one of the typical PDEs, which has been derived in 1976 by Kuramoto and Tsuzuki [34] as a model equation for interfacial instabilities in the context of angular phase turbulence for a system of a Reaction-diffusion equation that model the Belouzov-Zabotinskii reaction in three space dimensions, and independently, in 1977, by Sivashinsky [35] to model thermal diffusion instabilities observed in laminar Mame fronts in two space dimensions:

$$\frac{\partial \boldsymbol{X}}{\partial \boldsymbol{t}} + 4\frac{\partial^4 \boldsymbol{X}}{\partial \boldsymbol{z}^4} + \alpha\left[\frac{\partial^2 \boldsymbol{X}}{\partial \boldsymbol{z}^2} + \frac{1}{2}\left(\frac{\partial \boldsymbol{X}}{\partial \boldsymbol{z}}\right)^2\right] + \sum_{i=1}^{m} \boldsymbol{h}_i(\boldsymbol{z})\, \boldsymbol{u}_i(\boldsymbol{t}) = 0 \tag{62}$$

where $\alpha = 84.25$; $\boldsymbol{h}_i(\boldsymbol{z}) = \delta[\boldsymbol{z} + 3\pi/4 - (\boldsymbol{i}-1)\pi/2]$; $\boldsymbol{m} = 4$;

$$[\boldsymbol{u}_1(\boldsymbol{t}), \boldsymbol{u}_2(\boldsymbol{t}), \boldsymbol{u}_3(\boldsymbol{t}), \boldsymbol{u}_4(\boldsymbol{t})] = \left[5\cos\frac{\boldsymbol{t}}{4}, 5\sin\frac{\boldsymbol{t}}{4}, 5\cos\frac{\boldsymbol{t}}{2}, 5\sin\frac{\boldsymbol{t}}{2}\right]. \tag{63}$$

Equation (62) is subject to periodic boundary condition $\boldsymbol{X}(\boldsymbol{z}, \boldsymbol{t}) = \boldsymbol{X}(\boldsymbol{z} + 2\pi, \boldsymbol{t})$, and the initial condition is set to be $\cos z$. The sampling interval Δt is 0.001s and the simulation time is 0.5s. In this case, forty-one sensors uniformly distributed in the space are used for measurements. A noise dataset of 500 data is collected from (62). This size of data set used for training may be determined by the system complexity and the desired modelling accuracy. More complex system and higher accuracy requirements may need more data from the observation. The solutions of K-S Equation (62) are calculated using the same method in [28], and the performance of this method is compared with the improved EEFs proposed in [28]. After the initial EEFs are derived from the collected spatiotemporal data, a 5-order nonlinear ODE system can be obtained by time/space separation and Galerkin projection. According to the ODE system, coefficient matrix in (20) can be computed by the balanced realization and truncation for its empirical controllability and observability matrices. This computational approach is introduced by Juergen Hahn [29]. Thus, the modified EEFs can be obtained by linear combinations of initial EEFs. A new set of 100 data is collected for testing to compare the performances of two kinds of spatial basis functions (Figure 1). The spatiotemporal output of the K-S equation on testing data can be estimated from the synthesis of the temporal approximate model and spatial basis functions.

The first four initial EEFs capture over 99% of energy, the RMSEs of the approximate models based on the first four EEFs, and the first four improved EEFs, and the four modified EEFs are compared in Figure 2. The values of RMSE using modified EEFs are smaller than that using the same number of improved EEFs and also much smaller than that using initial EEFs. Because the improved and modified EEFs are derived from linear combinations of initial EEFs (the number is larger than their numbers), the dynamics of the neglectful modes are used to compensate the initial EEFs-based reduced models and then the modeling performance based on improved and modified EEFs is better than initial EEFs-based models. It is worth noticing that when three or four spatial basis functions are used to model reduction for nonlinear DPSs, their model accuracy is close. The reason

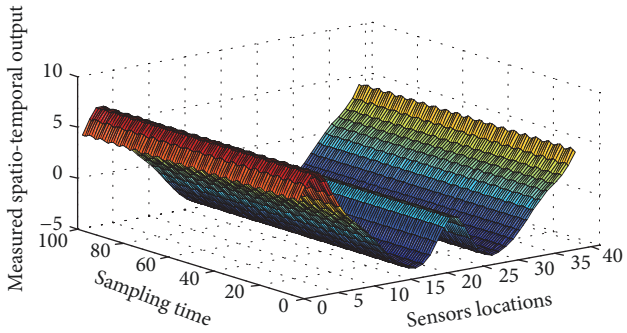

Figure 1: Measured spatiotemporal output for testing.

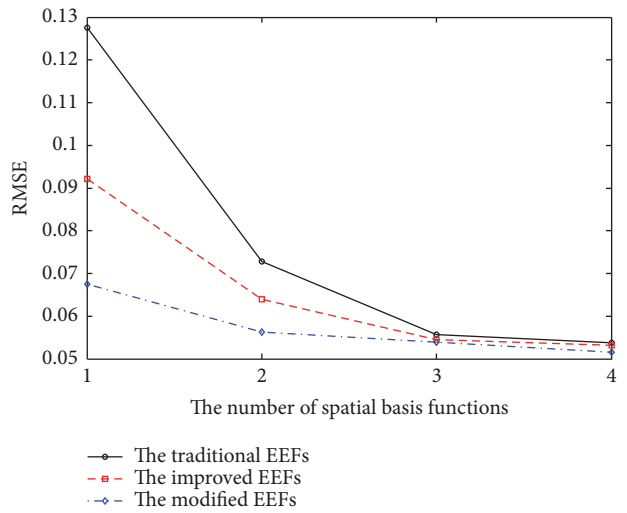

Figure 2: RMSEs based on traditional, improved and modified EEFs.

is that the dynamics information of the neglectful modes becomes much smaller for long-term behaviors and the compensations for the dynamics of the reduced model are restricted.

In order to demonstrate the performance of the modified EEFs clearly, model reduction performances by using the first two improved and modified EEFs on the testing data are compared. First, the two improved and modified EEFs are shown in Figures 3 and 5, respectively. The predicted spatiotemporal outputs based on two kinds of basis functions are given in Figures 4 and 6, respectively. Compared with the testing data, the predicted distribution errors based on two kinds of basis functions are shown in Figures 7 and 8, respectively. The RMSEs of the approximate model based on the two improved and modified EEFs are 0.0728 and 0.0563, respectively.

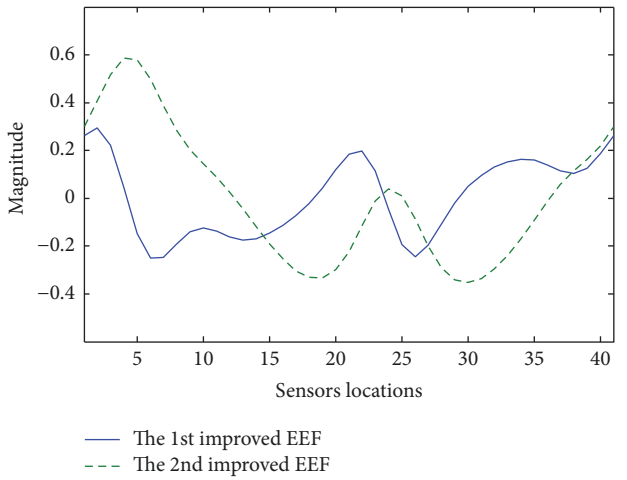

Figure 3: The first two improved EEFs in [28].

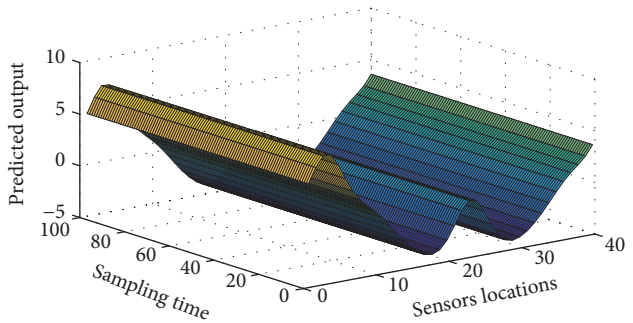

Figure 4: The predicted output based on two improved EEFs based modelling.

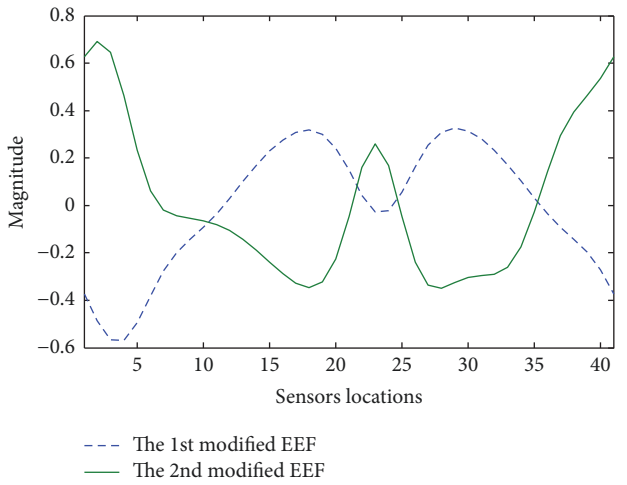

Figure 5: The first two modified EEFs.

Remarks. Nonlinear closure modeling [24, 25] also considered the influences of higher POD modes on the stability and accuracy of the reduced-order model in turbulent, which has shown promising results for Burger's equation and the Navier-Stokes equations. In its numerical examples, it can be found that the first several POD modes that capture over 99% of energy are used in model reduction will generate less accurate results for the cases. This illustrates the significant role of higher POD modes in the closure model, which improve the accuracy of the reduced order model. Unlike the nonlinear closure modeling approach, the method in this paper actually uses the linear combinations of initial

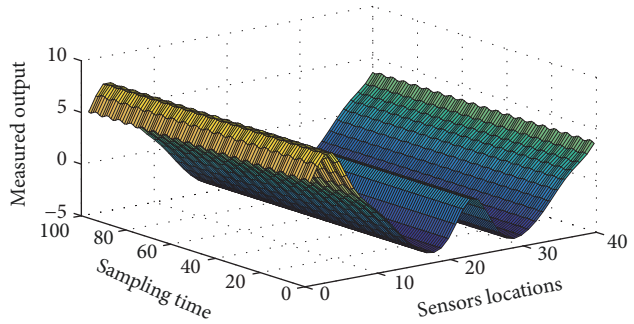

Figure 6: The predicted output based on two modified EEFs based modelling.

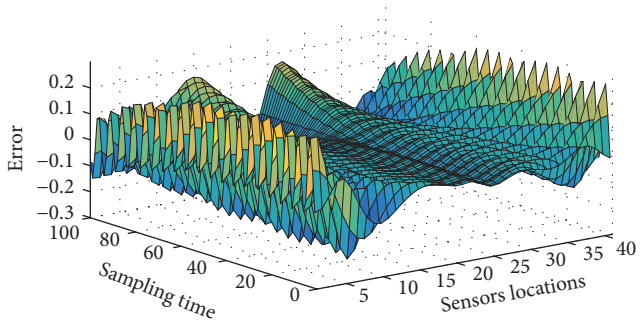

Figure 7: Distributed error based on two improved EEFs in [28].

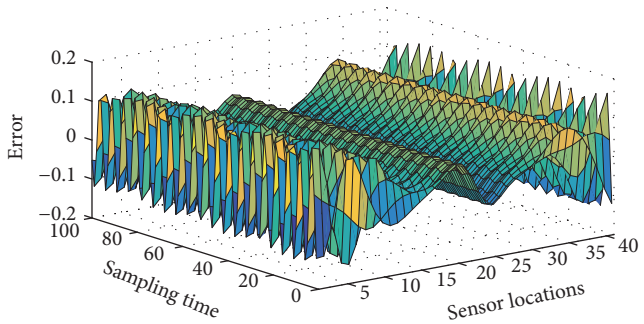

Figure 8: Distributed error based on two modified EEFs.

EEFs with more modes to obtain the modified EEFs with fewer modes, and the coefficients are derived from the temporal dynamics to introduce the information of higher modes to the reduced order model. The first couple of modes with 99% of energies are employed to demonstrate the compensation effects of higher modes on the reduced model. The influences by higher modes for dynamics of the reduced model can be found from the variations of RMSEs in Figure 2. However, to further improve the accuracy of the reduced model and optimize the proposed technique, more initial EEFs can be employed to generate the modified EEFs, which can be chosen arbitrarily according to its energies (i.e., all initial modes with non-zero energies are used for linear combinations). This will require higher computational costs to enhance the numerical accuracy. The comparisons with nonlinear closure modeling approach and the utilization of sensitivity analysis [21–23] to enhance the robustness of the reduced model will be carried out in our further research work, which deserve a long-term study.

6. Conclusions

In this paper, modified EEFs were proposed for model reduction of the nonlinear STSs, which were derived by adding an extra weight matrix in the method of snapshots. This transforms the derivation of modified EEFs to linear combinations of initial EEFs, while the coefficients matrix was computed according to the nonlinear temporal dynamics of STSs. Thus, the effects of high modes were considered into model reduction with less computational requirements, and the dimension of reduced model is smaller under a given accuracy. The performance of modified EEFs based model reduction is proved theoretically, which are compared with that of the traditional EEFs and the improved EEFs in [28] by a numerical example.

Appendix

The Karhunen–Loève expansion (also known as principal component analysis, principal orthogonal decomposition) is to find an optimal basis from a representative set of process data. Suppose that there is an observation $\{\boldsymbol{Y}(\boldsymbol{z}_i, \boldsymbol{t}_j) \mid \boldsymbol{z}_i \in \Omega,\ \boldsymbol{i} = 1, \cdots, \boldsymbol{M},\ \boldsymbol{j} = 1, \cdots, \boldsymbol{L}\}$ (called snapshots). The problem is how to compute the most characteristic structure $\varphi(\boldsymbol{z})$ among these snapshots $\boldsymbol{Y}(\boldsymbol{z}, \boldsymbol{t})$.

For simplicity, assume that the observations $\{\boldsymbol{Y}(\boldsymbol{z}_i, \boldsymbol{t}_j)\}$ are uniformly sampled in time and space. Defining the inner product, norm, and ensemble average as $(\boldsymbol{f}(\boldsymbol{z}), \boldsymbol{g}(\boldsymbol{z}))_\Omega = \int_\Omega \boldsymbol{f}(\boldsymbol{z})\boldsymbol{g}(\boldsymbol{z})d\boldsymbol{z}$, $\|\boldsymbol{f}(\boldsymbol{z})\| = (\boldsymbol{f}(\boldsymbol{z}), \boldsymbol{f}(\boldsymbol{z}))_\Omega^{1/2}$, and $\langle \boldsymbol{f}(\boldsymbol{z}, \boldsymbol{t})\rangle = (1/\boldsymbol{L}) \sum_{\boldsymbol{t}=1}^{\boldsymbol{L}} \boldsymbol{f}(\boldsymbol{z}, \boldsymbol{t})$.

Motivated by Fourier series, the spatiotemporal variable $\boldsymbol{Y}(\boldsymbol{z}, \boldsymbol{t})$ can be expanded onto an infinite number of orthonormal spatial basis functions $\{\varphi_i(\boldsymbol{z})\}_{i=1}^{\infty}$ with temporal coefficients $\{\boldsymbol{y}_i(\boldsymbol{t})\}_{i=1}^{\infty}$:

$$\boldsymbol{Y}(\boldsymbol{z}, \boldsymbol{t}) = \sum_{\boldsymbol{i}=1}^{\infty} \boldsymbol{y}_{\boldsymbol{i}}(\boldsymbol{t})\, \varphi_{\boldsymbol{i}}(\boldsymbol{z}). \tag{A.1}$$

The temporal coefficients can be computed from

$$\boldsymbol{y}_{\boldsymbol{i}}(\boldsymbol{t}) = \left(\phi_{\boldsymbol{i}}(\boldsymbol{z}), \boldsymbol{Y}(\boldsymbol{z}, \boldsymbol{t})\right)_\Omega, \quad \boldsymbol{i} = 1, 2, \cdots, \infty. \tag{A.2}$$

$\boldsymbol{Y}_{\boldsymbol{M}}(\boldsymbol{z}, \boldsymbol{t})$ denotes the $\boldsymbol{M}$-order approximation

$$\boldsymbol{Y}_{\boldsymbol{M}}(\boldsymbol{z}, \boldsymbol{t}) = \sum_{\boldsymbol{i}=1}^{\boldsymbol{M}} \boldsymbol{y}_{\boldsymbol{i}}(\boldsymbol{t})\, \varphi_{\boldsymbol{i}}(\boldsymbol{z}). \tag{A.3}$$

The main procedure of using Karhunen–Loève expansion for time/space separation is computing the most characteristic spatial structure $\{\varphi_i(\boldsymbol{z})\}_{i=1}^{\boldsymbol{M}}$ among the spatiotemporal output $\{\boldsymbol{Y}(\boldsymbol{z}_i, \boldsymbol{t}_j)\}_{i=1,j=1}^{\boldsymbol{M},\boldsymbol{L}}$. This typical structure can be found by minimizing the objective function

$$\begin{aligned} &\min_{\phi_i(\boldsymbol{z})} \quad \left\langle \left\| \boldsymbol{Y}(\boldsymbol{z}, \boldsymbol{t}) - \boldsymbol{Y}_{\boldsymbol{M}}(\boldsymbol{z}, \boldsymbol{t}) \right\|^2 \right\rangle \\ &\textbf{subject to} \quad (\varphi_i, \varphi_i) = 1, \quad \boldsymbol{i} = 1, \cdots, \boldsymbol{M}. \end{aligned} \tag{A.4}$$

The orthogonal constraint is imposed to ensure that the function $\varphi_i(z)$ is unique. The Lagrangian functional corresponding to this constrained optimization problem is

$$J = \left\langle \left\| Y(z,t) - Y_M(z,t) \right\|^2 \right\rangle + \sum_{i=1}^{M} \lambda_i \left[(\varphi_i, \varphi_i) - 1 \right]. \quad \text{(A.5)}$$

And the solution can be obtained as

$$\int_\Omega D(z,\xi)\,\varphi_i(z)\,d\xi = \lambda_i \varphi_i(z), \quad (\varphi_i, \varphi_i) = 1, \ i = 1, \cdots, M, \quad \text{(A.6)}$$

where $D(z,\xi) = \langle Y(z,t) Y(\xi,t) \rangle$ is the spatial two-point correlation function. $\varphi_i(z)$ is the ith eigenfunction, and λ_i is the corresponding eigenvalue. Given that the covariance matrix λ_i is symmetric and positive definite, its eigenvalues λ_i are real and its eigenvectors $\varphi_i(z)$, $i = 1, 2, \cdots, M$, form an orthogonal set. Since the data are always discrete in space, one must numerically solve the integral (A.6). Discretizing the integral equation gives a $M \times M$ matrix eigenvalue problem. Thus, at most M eigenfunctions at M sampling spatial locations can be obtained.

The maximum number of nonzero eigenvalues is $n = \min(M, L)$. We arrange the eigenvalues $\lambda_1 > \lambda_2 > \cdots > \lambda_n$ and $\varphi_1(z), \varphi_2(z), \cdots, \varphi_n(z)$, in order of the magnitude of the eigenvalues. Each eigenfunction has an energy percentage which depends on the associated eigenvalues of the eigenfunctions:

$$F_k = \frac{\lambda_k}{F} \quad \text{(A.7)}$$

where $F = \sum_{i=1}^{n} \lambda_i$ denotes the sum of the matrix eigenvalues. Assuming that the eigenvalues are sorted in descending order, the eigenfunctions are ordered from most to least energetic. In general, an expansion in terms of only the first few temporal coefficients

$$Y_n(z,t) = \sum_{i=1}^{n} y_i(t)\,\varphi_i(z) \quad \text{(A.8)}$$

can be used to represent the dominant dynamics of DPSs. The common model reduction can be accomplished for the nonlinear DPSs based on the initial EEFs.

Data Availability

The MATLAB programs for the data of the numerical example used to support the findings of this study are available from the corresponding author upon request.

Conflicts of Interest

The authors declare that there are no conflicts of interest regarding the publication of this paper.

Acknowledgments

This project is supported by National Natural Science Foundation of China (Grant nos. 51775182, 51775181). Natural Science Foundation of Hunan province (Grant no. 2018JJ3170) and the Outstanding Youth Fund of the Education Department of Hunan Province (Grant no. 16B093) are also gratefully acknowledged.

References

[1] H. Park and D. Cho, "The use of the Karhunen-Loève decomposition for the modeling of distributed parameter systems," *Chemical Engineering Science*, vol. 51, no. 1, pp. 81–98, 1996.

[2] C. K. Qi, H.-X. Li, S. Y. Li, X. Zhao, and F. Gao, "A fuzzy-based spatio-temporal multi-modeling for nonlinear distributed parameter processes," *Applied Soft Computing*, vol. 25, pp. 309–321, 2014.

[3] C. K. Qi, H. X. Li, S. Li et al., "Probabilistic PCA-based Spatiotemporal Multi-modeling for Nonlinear Distributed Parameter Processes," *Industrial & Engineering Chemistry Research*, vol. 51, no. 19, pp. 6811–6822, 2012.

[4] C. K. Qi, H.-X. Li, S. Li et al., "Kernel-Based Spatiotemporal Multi-modeling for Nonlinear Distributed Parameter Industrial Processes," *Industrial & Engineering Chemistry Research*, vol. 51, no. 40, pp. 13205–13218, 2012.

[5] J. Wu, M. Jiang, X. Li, and H. Feng, "Assessment of severity of nonlinearity for distributed parameter systems via nonlinearity measures," *Journal of Process Control*, vol. 58, pp. 1–10, 2017.

[6] X. Lu, W. Zou, and M. Huang, "A novel spatiotemporal LS-SVM method for complex distributed parameter systems with applications to curing thermal process," *IEEE Transactions on Industrial Informatics*, vol. 12, no. 3, pp. 1156–1165, 2016.

[7] X. Lu, F. Yin, C. Liu, and M. Huang, "Online Spatiotemporal Extreme Learning Machine for Complex Time-Varying Distributed Parameter Systems," *IEEE Transactions on Industrial Informatics*, vol. 13, no. 4, pp. 1753–1762, 2017.

[8] X. Lu, F. Yin, and M. Huang, "Online Spatiotemporal Least-Squares Support Vector Machine Modeling Approach for Time-Varying Distributed Parameter Processes," *Industrial & Engineering Chemistry Research*, vol. 56, no. 25, pp. 7314–7321, 2017.

[9] S. L. Brunton and B. R. Noack, "Closed-loop turbulence control: Progress and challenges," *Applied Mechanics Reviews*, vol. 67, no. 5, pp. 1–48, 2015.

[10] K.-K. Xu, H.-X. Li, and Z. Liu, "ISOMAP-based spatiotemporal modeling for lithium-ion battery thermal process," *IEEE Transactions on Industrial Informatics*, vol. 14, no. 2, pp. 569–577, 2018.

[11] K. Xu, H. Li, and H. Yang, "Local-Properties-Embedding-Based Nonlinear Spatiotemporal Modeling for Lithium-Ion Battery Thermal Process," *IEEE Transactions on Industrial Electronics*, vol. 65, no. 12, pp. 9767–9776, 2018.

[12] B. Luo, H.-N. Wu, and H.-X. Li, "Data-based suboptimal neurocontrol design with reinforcement learning for dissipative spatially distributed processes," *Industrial & Engineering Chemistry Research*, vol. 53, no. 19, pp. 8106–8119, 2014.

[13] N. Aubry, W. Y. Lian, and E. S. Titi, "Preserving symmetries in the proper orthogonal decomposition," *SIAM Journal on Scientific Computing*, vol. 14, no. 2, pp. 483–505, 1993.

[14] D. Armbruster, R. Heiland, E. J. Kostelich, and B. Nicolaenko, "Phase-space analysis of bursting behavior in Kolmogorov flow," *Physica D: Nonlinear Phenomena*, vol. 58, no. 1-4, pp. 392–401, 1992.

[15] B. R. Noack, K. Afanasiev, M. Morzynski, G. Tadmor, and F. Thiele, "A hierarchy of low-dimensional models for the transient and post-transient cylinder wake," *Journal of Fluid Mechanics*, vol. 497, pp. 335–363, 2003.

[16] T. K. Sengupta, N. Singh, and V. K. Suman, "Dynamical system approach to instability of flow past a circular cylinder," *Journal of Fluid Mechanics*, vol. 656, pp. 82–115, 2010.

[17] S. Ahuja, C. Rowley, I. Kevrekidis, M. Wei, T. Colonius, and G. Tadmor, "Low-Dimensional Models for Control of Leading-Edge Vortices: Equilibria and Linearized Models," in *Proceedings of the 45th AIAA Aerospace Sciences Meeting and Exhibit*, Reno, Nev, USA, January, 2007.

[18] M. Bergmann, C.-H. Bruneau, and A. Iollo, "Enablers for robust POD models," *Journal of Computational Physics*, vol. 228, no. 2, pp. 516–538, 2009.

[19] S. Sirisup and G. E. Karniadakis, "A spectral viscosity method for correcting the long-term behavior of POD models," *Journal of Computational Physics*, vol. 194, no. 1, pp. 92–116, 2004.

[20] Z. Wang, I. Akhtar, J. Borggaard, and T. Iliescu, "Proper orthogonal decomposition closure models for turbulent flows: a numerical comparison," *Computer Methods Applied Mechanics and Engineering*, vol. 237/240, pp. 10–26, 2012.

[21] A. Hay, I. Akhtar, and J. T. Borggaard, "On the use of sensitivity analysis in model reduction to predict flows for varying inflow conditions," *International Journal for Numerical Methods in Fluids*, vol. 68, no. 1, pp. 122–134, 2012.

[22] I. Akhtar, J. Borggaard, and A. Hay, "Shape Sensitivity Analysis in Flow Models Using a Finite-Difference Approach," *Mathematical Problems in Engineering*, vol. 2010, Article ID 209780, 22 pages, 2010.

[23] A. Hay, J. Borggaard, I. Akhtar, and D. Pelletier, "Reduced-order models for parameter dependent geometries based on shape sensitivity analysis," *Journal of Computational Physics*, vol. 229, no. 4, pp. 1327–1352, 2010.

[24] H. Imtiaz and I. Akhtar, "Closure modeling in reduced-order model of Burgers' equation for control applications," *Proceedings of the Institution of Mechanical Engineers, Part G: Journal of Aerospace Engineering*, vol. 231, no. 4, pp. 642–656, 2017.

[25] I. Akhtar and A. H. Nayfeh, "Model Based Control of Laminar Wake Using Fluidic Actuation," *Journal of Computational and Nonlinear Dynamics*, vol. 5, no. 4, p. 041015, 2010.

[26] W. Kang, J.-Z. Zhang, S. Ren, and P.-F. Lei, "Nonlinear Galerkin method for low-dimensional modeling of fluid dynamic system using POD modes," *Communications in Nonlinear Science and Numerical Simulation*, vol. 22, no. 1-3, pp. 943–952, 2015.

[27] N. H. El-Farra, M. A. Demetriou, and P. D. Christofides, "Actuator and controller scheduling in nonlinear transport-reaction processes," *Chemical Engineering Science*, vol. 63, no. 13, pp. 3537–3550, 2008.

[28] M. Jiang and H. Deng, "Improved empirical eigenfunctions based model reduction for nonlinear distributed parameter systems," *Industrial & Engineering Chemistry Research*, vol. 52, no. 2, pp. 934–940, 2013.

[29] J. Hahn and T. F. Edgar, "Balancing approach to minimal realization and model reduction of stable nonlinear systems," *Industrial & Engineering Chemistry Research*, vol. 41, no. 9, pp. 2204–2212, 2002.

[30] S. Lall, J. E. Marsden, and S. Glavaski, "A subspace approach to balanced truncation for model reduction of nonlinear control systems," *International Journal of Robust and Nonlinear Control*, vol. 12, no. 6, pp. 519–535, 2002.

[31] M. Jiang, J. Wu, W. Zhang, and X. Li, "Empirical Gramian-based spatial basis functions for model reduction of nonlinear distributed parameter systems," *Mathematical and Computer Modelling of Dynamical Systems. Methods, Tools and Applications in Engineering and Related Sciences*, vol. 24, no. 3, pp. 258–274, 2018.

[32] B. C. Moore, "Principal component analysis in linear systems: controllability, observability, and model reduction," *IEEE Transactions on Automatic Control*, vol. 26, no. 1, pp. 17–32, 1981.

[33] K. Zhou and J. C. Doyle, *Essentials of Robust Control*, Prentice Hall, Englewood: Cliffs, NJ, USA, 1998.

[34] Y. Kuramoto and T. Tsuzuki, "Persistent Propagation of Concentration Waves in Dissipative Media Far from Thermal Equilibrium," *Progress of Theoretical and Experimental Physics*, vol. 55, no. 2, pp. 356–369, 1976.

[35] G. I. Sivashinsky, "Nonlinear analysis of hydrodynamic instability in laminar flames. I. Derivation of basic equations," *Acta Astronautica*, vol. 4, no. 11-12, pp. 1177–1206, 1977.